Improving the representation of internal nutrient recycling with phosphorus mass balance models: A case study in the Bay of Quinte, Ontario, Canada

Dong-Kyun Kim [a], Weitao Zhang [a], Yerubandi R. Rao [b], Sue Watson [b], Shan Mugalingam [c], Tanya Labencki [d], Maria Dittrich [a], Andrew Morley [e], George B. Arhonditsis [a,*]

[a] Ecological Modelling Laboratory, Department of Physical and Environmental Sciences, University of Toronto, Toronto, Ontario, Canada M1C 1A4
[b] Environment Canada, National Water Research Institute, Burlington, Ontario, Canada L7R 4A6
[c] Lower Trent Conservation, Trenton, Ontario, Canada K8V 5P4
[d] Environmental Monitoring and Reporting Branch, Ontario Ministry of the Environment, Toronto, Ontario, Canada M9P 3V6
[e] Kingston Regional Office, Ontario Ministry of the Environment, Kingston, Ontario, Canada K7M 8S5

ABSTRACT

We evaluate the relative importance of the causal connection between exogenous total phosphorus (*TP*) loading and internal nutrient recycling with the water quality conditions in the Bay of Quinte, Ontario, Canada. First, we examine the temporal trends of all the major point and non-point loading sources over the last four decades. We then enhance the mechanistic foundation of an existing simple mass-balance total phosphorus (*TP*) model, originally developed to guide the eutrophication management in the system. The structural improvements include the incorporation of macrophyte dynamics, the explicit representation of the role of dreissenids in the system, and the improved portrayal of the interplay between water column and sediments. The upgraded model was in good agreement with the observed *TP* variability in the system during the study period (2002–2009) and successfully reproduced the *TP* accumulation patterns toward the end of the summer-early fall. We provide evidence that phosphorus dynamics in the upper Bay are predominantly driven by the inflows from Trent River, while the middle and lower segments likely receive substantial internal subsidies from the sediment diagenesis mechanisms and/or the activity of macrophytes and dreissenids (e.g., pseudofeces production, nutrient pump effect). We also forced the model with scenarios of reduced nutrient loading and examine the likelihood of the system to meet its water quality delisting targets, although we caution that our complex overparameterized modeling construct is primarily intended for heuristic purposes. The present study together with the companion paper by Zhang et al. (2013) illustrate how phosphorus mass balance models can offer useful tools for improving our understanding of freshwater ecosystems.

© 2013 Elsevier B.V. All rights reserved.

1. Introduction

In many parts of the Laurentian Great Lakes, the arrival of dreissenid mussels has induced a major reengineering of the biophysical littoral environment with profound alterations on the retention and recycling of nutrients (Coleman and Williams, 2002). This nearshore shunt (sensu Hecky et al., 2004) is hypothesized to have modified the processing of particulate material in the littoral zones, with critical ramifications for their relative productivity and their interplay with the offshore areas. Depending on the concentration of food particles, dreissenid mussels can filter twice as much material as they actually ingest (Walz, 1978), and thus a large proportion is excreted in soluble form or released in particulate form

as either feces or pseudofeces. Given also that a significant portion of the latter particulate material is thought to be subsequently remineralized by the community of detritivores and decomposers, the contemporary literature hypothesized that dreissenids mediate the nutrient cycling and may significantly modulate the nearshore nutrient concentrations (Holland et al., 1995; James et al., 1997). Following the establishment of the causal link between dreissenids and nutrient variability in the littoral zone, Hecky et al. (2004) questioned the structural adequacy of the nutrient mass-balance models developed during the pre-dreissenid period in the Great Lakes. Because of their founding assumption that the lakes resemble well-mixed reactors, it was argued that the lack of discrimination between nearshore and offshore regions and the adoption of a lake-wide sedimentation rate to reproduce particle and nutrient removal from the water column will introduce systematic biases (Hecky et al., 2004). An additional problematic feature that undermines the suitability of simple mass balance phosphorus models as

---

* Corresponding author. Tel.: +1 416 208 4858; fax: +1 416 287 7279.
E-mail address: georgea@utsc.utoronto.ca (G.B. Arhonditsis).

management tools is their failure to explicitly consider the capacity of the nearshore shunt to shape the relationship between external loading and ecosystem response in both space and time.

In the Bay of Quinte, recent efforts have focused on the delineation of the ecological implications of the establishment of invasive zebra and quagga mussels in the mid-1990s relative to a substantial ($\approx$50%) reduction in the point-source phosphorus loading into the upper segments during the winter of 1977–1978 (Nicholls and Carney, 2011; Nicholls et al., 2002). Existing evidence suggests that the presence of dreissenid mussels in the system may have induced a series of cause–effect relationships that could be translated into an ecosystem regime shift (deYoung et al., 2008; Scheffer et al., 2001). Namely, contrary to the limited macrophyte response to the point-source phosphorus control, the significant increase of the light penetration, stemming from the filtration of lakewater by dreisseinds, is likely to have triggered the growth of submerged macrophytes and the rapid expansion of existing shallow-water beds into deeper water (Leisti et al., 2006; Seifried, 2002). Dreissenids can consume particles in a wide size range including microzooplankton (e.g., protozoa, ciliates, rotifers, veligers and nauplii), and thus may have shaped the zooplankton community structure in the Bay, such as the low rotifer biomass that represents less than 5% of the total zooplankton biomass (Bowen and Johannsson, 2011). Dreissenid-induced declines in larger zooplankton could indirectly occur through their impact on food abundance as well as through the changes in predation, as the increased water clarity leads to an easier detection by higher predators (Bowen and Johannsson, 2011).

With respect to the phytoplankton community response, Nicholls and Carney (2011) contended that the arrival of dreissenid mussels may be associated with both desirable (e.g., *Aphanizomenon* and *Oscillatoria* decline) and undesirable (e.g., *Microcystis* increase) changes in the trophic efficiency and ecosystem health integrity. In particular, the post-*Dreissena* increase of the cyanophyte *Microcystis* has significant implications for the esthetics and other beneficial uses in the Bay, through the formation of "scums" on the water surface (Jacoby et al., 2000) as well as due to the fact that some strains of *Microcystis* are toxin producers (Brittain et al., 2000; Vanderploeg et al., 2001), e.g., one of the most common species, *Microcystis aeruginosa*, is a producer of the hepatotoxin microcystin-LR (Repavich et al., 1990). Some of these structural changes in the phytoplankton community composition could stem directly from the feeding selectivity of dreissenids or indirectly from the improvements in the transparency of the water column, but the role of the feedback loop associated with their nutrient recycling activity could conceivably be another important factor (Bierman et al., 2005). Interestingly, total phosphorus concentrations in the post-dreissenid period demonstrate significant intra-annual variability, characterized by relatively low spring and autumn levels, 10–15 μg TPL^{-1}, and quite high summer concentrations, >50 μg TPL^{-1}, which exceed the targeted delisting criterion of 30 μg TPL^{-1} (Munawar et al., 2011). This pattern may reflect the regeneration of phosphorus from sedimented materials on the lake bottom, the gradual retention of particulate P as algal biomass or biological recycling activity.

In this study, we use mathematical modeling to test the hypothesis that the establishment of dreissenids and the resurgence of macrophytes may be causally linked with the end of summer-early fall TP accumulation in the Bay of Quinte. First, we present the structural augmentation of the eight-segment *TP* mass-balance model, originally developed by Minns and Moore (2004) and recently modified by Zhang et al. (2013). Improvements in the mechanistic foundation of the model include the incorporation of macrophyte dynamics, the explicit representation of the role of dreissenids in the system, and the improved portrayal of the interplay between water column and sediments. We provide the rationale behind the

model structure adopted, the simplifications included, and the formulations used during the development phase of the model. We then present the results of a calibration exercise and examine the ability of the model to sufficiently reproduce the observed patterns in the Bay of Quinte during the 2002–2009 study period. We also conduct a local sensitivity analysis to identify the most influential components of the model and to shed light on the spatiotemporal role of the various ecological processes and cause–effect relationships, as postulated by the present parameterization. Our modeling study also undertakes an estimation of the critical nutrient loads that will ultimately lead to compliance of the system with threshold levels of the ambient total phosphorus. Several of the lessons learned during the model calibration and sensitivity analysis are highlighted as pointers for future research and management actions in the Bay of Quinte.

2. Materials and methods

2.1. Dataset description

Daily inflows were based on daily discharge data obtained from Environment Canada (Water Survey Division, Burlington) for gauging stations on five rivers: Trent River, Moira River, Salmon River, Napanee River, and Wilton Creek (Fig. 1). Water quality data for the rivers were provided by the Provincial Water Quality Monitoring Network of Ontario Ministry of the Environment (MOE). The precipitation data used were obtained from Environment Canada (Environmental Services Branch, Burlington) for the weather station at Trenton, consisting of rain and total precipitation in tenths of millimeters. Atmospheric deposition was based on bulk precipitation chemistry data obtained from Environment Canada, comprising samples collected with several different types of samplers at Trenton, Kingston, and Point Petrie. Estimates of point source inputs were based on flows and final effluent *TP* concentrations from the Belleville, Trenton, CFB Trenton, Deseronto, Napanee, and Picton sewage treatment plants (*STP*s), along with the same information for various industrial inputs to the Bay of Quinte. Detailed description about the data compilation and the derivation of the point and non-point nutrient loading estimates can be found in Minns et al. (2004). All *TP* concentrations in the Bay were generated as time-weighted monthly means of data provided by the Project Quinte members (2011). Monthly mean nutrient concentrations for the Lake Ontario outlet basin were also provided by the DFO's Long-term Bio-monitoring (Bioindex) Program (Minns et al., 2004).
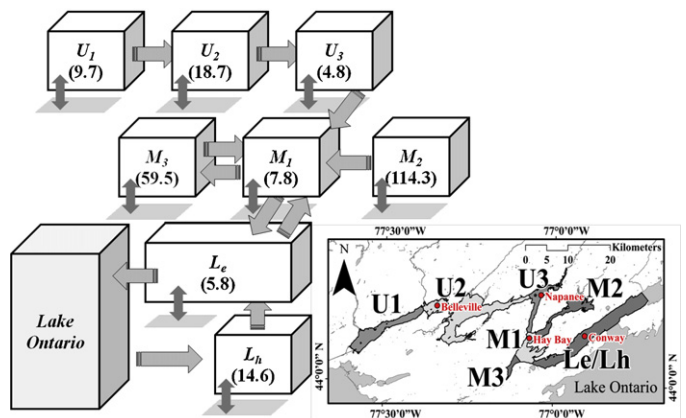

Fig. 1. Map of the Bay of Quinte (bottom right) and mass exchange patterns among the model segments. Numbers in the brackets correspond to the average flushing rate of each segment. Small dark-gray arrows denote settling and sediment resuspension, while large light-gray arrows denote inflows, outflows, and backflows.

2.2. Dynamic Linear Modeling

Dynamic Linear Modeling analysis was used to examine the temporal trends of the riverine *TP*, while explicitly accounting for the fact that the flow can significantly covary with the *TP* concentrations. The main advantage of the *DLM*s is the explicit recognition of structure in the time series, i.e., the data are sequentially ordered and the level of the response variable at each time step is related to its levels at earlier time steps in the data series (Lamon et al., 1998; Stow et al., 2004). In contrast with regression analysis, in which each observation contains information on each parameter, *DLM* parameter estimates are influenced only by prior and current information, not by subsequent data. Parameter values are dynamic and reflect shifts in both the level of the response variable and the underlying ecological processes. *DLM*s easily handle missing values/unequally spaced data, and minimize the effect of outliers (Pole et al., 1994). All *DLM*s consist of an observation equation and system equations (West and Harrison, 1989). We parameterized these equations for the present study as follows:

Observation equation:

$$\ln[TP]_{ti} = level_t + \beta_t \ln[flow]_{ti} + \psi_{ti} \quad \psi_{ti} \sim N[0, \Psi_t]$$

System equations:

$$level_t = level_{t-1} + rate_t + \omega_{t1} \quad \omega_{t1} \sim N[0, \Omega_{t1}]$$

$$rate_t + rate_{t-1} + \omega_{t2} \quad \omega_{t2} \sim N[0, \Omega_{t2}]$$

$$\beta_t + \beta_{t-1} + \omega_{t3} \quad \omega_{t3} \sim N[0, \Omega_{t3}]$$

$$1/\Omega_{tj}^2 = \zeta^{t-1} \cdot 1/\Omega_{1j}^2, \ 1/\Psi_t^2 = \zeta^{t-1} \cdot 1/\Psi_1^2 \quad t > 1 \text{ and } j = 1 \text{ to } 3$$

$$level_1, \ rate_1, \ \beta_1 \sim N(0, 10000) \quad t = 1$$

$$1/\Omega_{tj}^2, \ 1/\Psi_t^2 \sim gamma(0.001, 0.001)$$

where $\ln[TP]_{ti}$ is the observed $\ln TP$ concentration at time t in the individual sample i, $level_t$ is the mean *TP* concentration at time t when accounting for the covariance with the flow, $\ln[flow]_{ti}$ is the observed standardized flow at time t in the individual sample i, $rate_t$ is the rate of change of the level variable, and β_t is a flow (regression) coefficient;. ψ_{ti}, ω_{t1}, ω_{t2}, and ω_{t3} are draws from normal distributions with zero mean values and variances of Ψ_t^2, Ω_{t1}^2, Ω_{t2}^2, and Ω_{t3}^2, respectively; the discount factor ζ represents the aging of information with the passage of time; $N(0,10000)$ is the normal distribution with mean 0 and variance 10000; and $gamma(0.001, 0.001)$ is the gamma distribution with shape and scale parameters of 0.001. The prior distributions for the parameters of the initial year $level_1$, $rate_1$, β_1, $1/\Omega_{1j}^2$, and $1/\Psi_1^2$ are considered "non-informative" or vague. The *DLM* process makes a forecast for time t based on prior knowledge of the parameters, and then we observe data at time t. Based on Bayes' Theorem, our knowledge regarding the parameters is updated using the likelihood of the data and our prior knowledge (Gelman et al., 2004). This posterior (updated) information about the parameters is "discounted" by adding a stochastic disturbance term to represent the aging of information with the passage of time. In this study, we introduce non-constant and data-driven variances (with respect to time) using a discount factor on the first period prior (Congdon, 2001). We examined different discounts between 0.8 and 1.0 (i.e., the static regression model) and the results reported here are based on a discount value of 0.95. This discounted posterior knowledge becomes prior knowledge for time $t + 1$, and the process is repeated.

2.3. Model description

The basis of the present study is the *TP* mass-balance model for the Bay of Quinte, originally developed by Minns and Moore
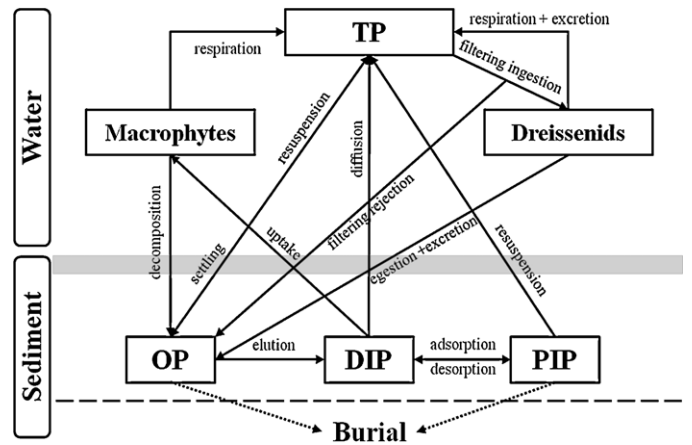

Fig. 2. Conceptual diagram of phosphorus mass transfer among the water column, macrophytes, dreissenids, and sediments. The gray bar represents the boundary between water column and sediments, and the dash line is the boundary between top and deep sediment layers.

(2004) and recently modified by Zhang et al. (2013). Improvements in the mechanistic foundation of that model involve the explicit representation of: (*i*) macrophyte dynamics, (*ii*) the role of dreissenids in the system, and (*iii*) several processes related to the fate and transport of phosphorus in the sediments along with the interplay between water column and sediments, such as particulate sedimentation dependent upon the standing algal biomass, sediment resuspension, sorption/desorption in the sediment particles, and organic matter decomposition. Schematic illustration of the processes considered in our study is provided in Fig. 2. This section is focused on the description of the basic conceptual design of the model. The mathematical formulations of the total phosphorus model are presented in Table 1 in the Supporting Information section (or Table SI-1), while all the state variables and parameter definitions are presented in Table SI-2.

2.3.1. Macrophyte submodel

The governing equation for macrophyte biomass considers production and losses due to respiration and mortality. Phosphorus and light impacts on macrophyte growth are included using a multiplicative model (Asaeda et al., 2000). Amongst the variety of mathematical formulations relating photosynthesis and light intensity, we used a light saturation curve along with Beer's law to scale photosynthetically active radiation to depth (Jassby and Platt, 1976). The extinction coefficient is determined as the sum of the background light attenuation and attenuation due to chlorophyll *a*. The macrophyte gross growth rate is modulated by phosphorus concentrations in the interstitial water of the sediments, using a Michaelis–Menten equation (Asaeda et al., 2000). Macrophyte biomass losses include all metabolic processes (respiration, excretion) as well as natural mortality; both processes were assumed to increase with temperature, described by the Arrhenius equation (Chapra, 1997). The main difference is that while the metabolic by-products are mainly released in the overlying waters, the dead plant tissues were assumed to fuel solely the sediment phosphorus pool.

2.3.2. Dreissenid submodel

Drawing parallels with the modeling approach presented by Bierman et al. (2005), the impact of dreissenids on water quality is represented by filtration of particulate material from the water column, and excretion of dissolved nutrients (Fig. 2). Dreissenid mussel filtering rate (FR) represents the volume of water swept clear of particles per unit time, and is maintained at a maximum

Table 1
Calibration vector of the Bay of Quinte TP model.

Symbol	Variables and parameters	Value	Unit
b_c	Exponent for weight effect on dreissenid ingestion	−0.39	
BP_{mac}	Phosphorus content in macrophyte biomass	0.0025	g P g dry weight^{-1}
BP_{zm}	Phosphorus content in dreissenid biomass	0.01	g P g dry weight^{-1}
b_r	Exponent for weight effect on respiration	−0.25	
b_{sdR}	Sediment bed shear stress exponent	1	
D_{mac}	Macrophyte mortality rate	0.001	day^{-1}
E	Langmuir sorption constant	9.5	L mg^{-1}
$f_{OP\text{-}ZM}$	Fraction of organic phosphorus in dreissenid excretion	0.6	
f_{resus}	Inorganic fraction of resuspended phosphorus	0.5	
I_{opt}	Optimal solar radiation for macrophyte growth	18	MJ m^{-2} day^{-1}
I_{zm}	Dreissenid food ingestion		g food g mussel^{-1} day^{-1}
K_1	Empirical coefficient representing temperature effect on ingestion at t_1	0.1	
K_2	Empirical coefficient representing temperature effect on ingestion at t_2	0.98	
K_3	Empirical coefficient representing temperature effect on ingestion at t_3	0.98	
K_4	Empirical coefficient representing temperature effect on ingestion at t_4	0.02	
K_{ad}	First-order desorption/sorption rate	7.2	day^{-1}
K_{cp}	Saturation particulate phosphorus concentration	50	μg P L^{-1}
K_{d20}	Decomposition rate coefficients at 20 °C	0.0002 (0.00018[b])	day^{-1}
K_{diff}	Sediment diffusion exchange at reference temperature (20 °C)	0.0007 (0.0003[b])	m^2 day^{-1}
K_{DO}	Half saturation constant for anaerobic phosphorus sediment release	0.5	mg O$_2$ L^{-1}
K_{nstr}	Diffusivity in non-stratified conditions	10	m^2 day^{-1}
K_p	Half saturation constant for phosphate in sediment pore water	10 (8.5[b])	μg L^{-1}
K_{str}	Diffusivity in stratified conditions	0.15	m^2 day^{-1}
PIP_{max}	Maximum sorption capacity	0.8	mg g^{-1}
P_m	Maximum gross photosynthesis rate	0.065 (0.052[b])	day^{-1}
Q	Slope estimate, approximately Q_{10}	3.1	
R_{mac20}	Macrophyte respiration rate at 20 °C	0.018 (0.0142[b])	day^{-1}
S_{bur}	Burial coefficient	5.86×10^{-6} (1×10^{-6}[b])	m day^{-1}
SDA	Fraction of ingestion spent on feeding energy	0.285	
t_0	Optimum temperature for standard respiration	28	°C
t_1	Lower temperature at which consumption is $K_1 \times$ maximum ingestion	2	°C
t_2	Lower temperature at which consumption is $K_2 \times$ maximum ingestion	12	°C
t_3	Higher temperature at which consumption is $K_3 \times$ maximum ingestion	21	°C
t_4	Higher temperature at which consumption is $K_4 \times$ maximum ingestion	32	°C
t_m	Maximum temperature for standard respiration	31	°C
w_f	Conversion efficiency	1.724	g mussel g food^{-1}
w_r	Respiration efficiency	5.586	g mussel g O$_2$ $^{-1}$
Z_{mac}	Water depth from the surface to the top of macrophyte bed	4.3	m
α_1	Background extinction coefficient	1	m^{-1}
α_2	Phytoplankton self-shading effect	0.02	m^2 mg chla^{-1}
α_c	Maximum dreissenid ingestion rate	0.031	g food g mussel^{-1} day^{-1}
α_f	Minimum fraction of food egested	0.315 (0.079[a])	
α_r	Maximum dreissenid respiration rate	0.002	g O$_2$ g mussel^{-1} day^{-1}
α_{sdR}	Resuspension coefficient	8	mg P m^2 day^{-1}
α_u	Fraction of assimilated food excreted	0.064	
γ_f	Coefficient for egestion dependence on food availability	0.88 (0.22[a])	
θ_d	Temperature coefficient for decomposition	1.08	
θ_{rmac}	Temperature dependence of macrophyte respiration	1.08	
θ_s	Temperature dependence of sediment diffusion	1.08	
τ_c	Critical sediment bed shear stress	0.03	N m^{-2}
φ	Sediment porosity	0.8	

[a] Dreissenid characterization that postulates more efficient feeding habits and lower dependence on food availability in the lower segment of the Bay of Quinte.

[b] Model parameterization based on the assumption that the current estimates underestimate by half the actual TP loading during the 2002–2009 period.

value for all food levels less than the saturation food concentration. Following Sprung and Rose (1988), the filtration rate is negatively related to food concentrations above that threshold value. The difference between the particulate material filtered and the mass actually ingested represents the production of pseudofeces. Our model also postulates that pseudofeces production is typically double the ingestion rate at high food concentrations, i.e., 34% of all food filtered is consumed and 66% is rejected as pseudofeces (Walz, 1978). Ingestion rate of an individual mussel is determined from its weight, temperature, and food availability. Ingestion is directly proportional to the particle content of the water for all food concentrations less than a threshold value, and remains constant at a maximum value when this saturation level is exceeded. A power function is used to model the inverse relationship between the weight of an individual mussel and its ingestion rate. Optimal food consumption occurs between 12 and 20 °C, with decreasing

consumption for temperatures above and below this range (Schneider, 1992; Thornton and Lessem, 1978). Respiration consists of a standard respiration rate and an energetic cost of feeding that is applied to the portion of food that is not egested (Bierman et al., 2005). According to our model, maximum respiration occurs at a temperature of 28 °C, while the upper lethal temperature was set equal to 31 °C (Schneider, 1992). Egestion is modeled as a function of ingestion, a minimum fraction of food egested, and a prespecified dependence on food availability (Schneider, 1992). The excreted material is modeled as a constant fraction of the assimilated food. Counter to the Bierman et al. (2005) study, our approach does not explicitly consider age cohort classes, while the effect of the entire dreissenid mussel population on particulate phosphorus concentration is obtained by multiplying the areal biomass estimates derived by our model with a used-specified colonization area.

2.3.3. Sediment submodel

The conceptual model of the interplay among the mechanisms involved in sediment phosphorus dynamics is provided in Fig. 2. Modeled phosphorus comprises three forms: dissolved inorganic phosphorus (DIP), exchangeable particulate phosphorus (PIP), and organic phosphorus (OP). The sediment–water column interactions take place within an "active layer" in the sediments, and its thickness is delineated by the penetration depth of oxygen (Wang et al., 2003a,b). Being the remnant of algae and other particulate matter (macrophyte dead tissues, dreissenid egested/excreted material) that have been deposited onto the sediment surface, organic phosphorus is transported toward the deeper sediments through burial. Temperature-dependent biological decomposition of organic phosphorus occurs in the sediments, whereby dissolved reactive phosphorus is regenerated. Dissolved phosphorus is subjected to diffusion, adsorption–desorption to/from the sediment particles, and burial. The release rate of dissolved phosphorus from the surface layer into the overlying water is modulated by the corresponding concentration gradients, the dissolved oxygen availability, and temperature. The latter two processes are in turn mathematically represented by the Michaelis–Menten and Arrhenius equations, respectively. Exchangeable particulate phosphorus may act as a sink or source for phosphorus, depending on the difference between the concentration in interstitial waters and a dynamic equilibrium concentration of dissolved phosphorus. The latter concentration was estimated from the exchangeable particulate phosphorus in sediments, assuming nonlinear sorption partitioning described by the Langmuir isotherm (Wang et al., 2003a,b). The burial fluxes of dissolved and particulate phosphorus from the active layer to the deeper parts of the sediments are directly proportional to their sediment concentrations.

Sediment resuspension is another potentially important sink of the phosphorus pool in the Bay of Quinte sediments, particularly in the shallow upper and middle segments. Sediment erosion depends strongly upon the magnitude of the bottom shear stress (Lick, 1986; Mehta et al., 1982; Tsai and Lick, 1986). In the present study, we used an empirical expression that postulates a linear relationship between sediment resuspension rate and the excess bed shear stress (Chao et al., 2008; Mehta et al., 1982). We also assumed that the bottom shear stress associated with the near-bed wave velocity is much larger than that associated with the near-bed current velocity (Mian and Yanful, 2004). The Sverdrup–Munk–Bretschneider (SMB) method for shallow water bodies was used to quantify the bed shear stresses, as a function of the wave characteristics (height, period length), the water depth, the wind speed and fetch length (CERC, 1994).

3. Results and discussion

3.1. Temporal trends of exogenous TP loading

We used DLM analysis to evaluate the temporal trends of the TP concentrations in five tributaries of the Bay of Quinte. First, we note the substantial within-year variability of the riverine TP concentrations until the mid-90s and their gradual stabilization since then (left panels in Fig. 3). In particular, there were occasions in the 1970s and 1980s, when the TP values in Salmon and Napanee Rivers exceeded the level of $250 \, \mu g \, L^{-1}$. Second, the mean annual TP concentrations have been declining over the last four decades, although our analysis reveals a recent shift to positive rates of change in some rivers (e.g., Trent, Salmon, and Napanee) which in turn are indicative of increasing trends in the corresponding TP concentrations (right panels in Fig. 3).

In Trent River, the mean annual TP concentrations have been gradually decreasing from their highest levels between 1965 and 1970 (ca. $50 \, \mu g \, L^{-1}$) to their lowest levels in 2000 (ca. $10 \, \mu g \, L^{-1}$). Yet, the earlier negative rates of change ($\mu g \, TP \, L^{-1} \, year^{-1}$) have switched to positive ones after 2003, providing evidence that the mean TP levels are rebounding after the second half of the last decade. In particular, the probability distribution that represents our knowledge of the annual rate of change indicates the odds of a negative rate of change were 2.3:1 in 1996, while a similar distribution derived from 2008 suggests that the odds of a positive rate are 1.8:1. [Note that the odds ratio of the annual rate of change being below zero in a particular year is the ratio of the probability mass below zero to the mass above zero.] The recent trends in Trent River may be partly associated with the variability of the ambient TP levels in the Kawartha Lakes (Lake Scugog, Lake Sturgeon and Pigeon Lake), located at the upper part of the Trent watershed (Alexander Shulyarenko, personal communication). Another plausible explanation may be related to the factors (e.g., meteorological patterns, runoff intensity, agricultural practices) that may be driving the recent phosphorus loading trends in the Lake Erie watershed (Ohio EPA, 2010; Palmer et al., 2011). For example, even though the total area used for farming declined in 2006 relative to 2001, the area undergoing tilling practices and receiving commercial fertilizer as input has increased. Further, agricultural areas appear to be undergoing consolidation and becoming part of larger sized farms (http://www.statcan.gc.ca/ca-ra2011/index-eng.htm). In a similar manner, the rates of change of the annual TP concentrations in Salmon River demonstrate a consistent decline until the mid-1990s and a slight increase thereafter. The Napanee River is characterized by the highest TP concentrations among the five rivers and the posterior predictive intervals of the DLM were also wider than any of the rivers studied. The mean annual TP concentrations were fluctuating throughout the 1970s and 1980s, followed by a decreasing trend and a gradual stabilization of their values ever since. Namely, the probability distribution of the rate of change indicates a <50% probability that it is still negative after 2001, while a similar distribution derived from 1990 suggests that the odds of a negative rate were 4.6:1. Finally, the TP levels follow a monotonic decreasing trajectory in Moira River and Wilton Creek throughout the study period.

Interesting temporal trends were also found in regards to the relative contribution of the different point and non-point sources to the total phosphorus loading in the Bay of Quinte (Fig. 4). Prior to the reduction of phosphorus in detergents and the upgrades at the local wastewater treatment plants in the 1970s, the inflows from Trent River represented less than 50% of the total loading discharges into the system. Yet, despite the aforementioned decline in the corresponding TP concentrations, the relative contribution of Trent River has gradually increased up to 70% over the last decade. By contrast, the proportion of phosphorus loading associated with the point sources was reduced from 21% to 3%, while the relative contribution of the rest of the tributaries has remained practically unaltered over the time-span examined. Importantly, recent empirical evidence suggests that the potential magnitude of the TP contribution from the un-gauged subwatersheds as well as the direct storm sewer discharges have been overlooked (XCG Consultants Ltd., 2009). Thus, given that their estimation is collectively based on the Wilton Creek equivalents (WCE) approach (see companion paper by Zhang et al., 2013), we caution that the absolute and relative role of the inflows from these sources is likely to be a major source of uncertainty of the present assessment.

In the context of eutrophication management, it is recognized that the sole consideration of the total annual P loading may be misleading when applied to highly flushed systems, like the Bay of Quinte (Minns et al., 2004). In this regard, we calculated the net loading from both point and non-point sources to weigh
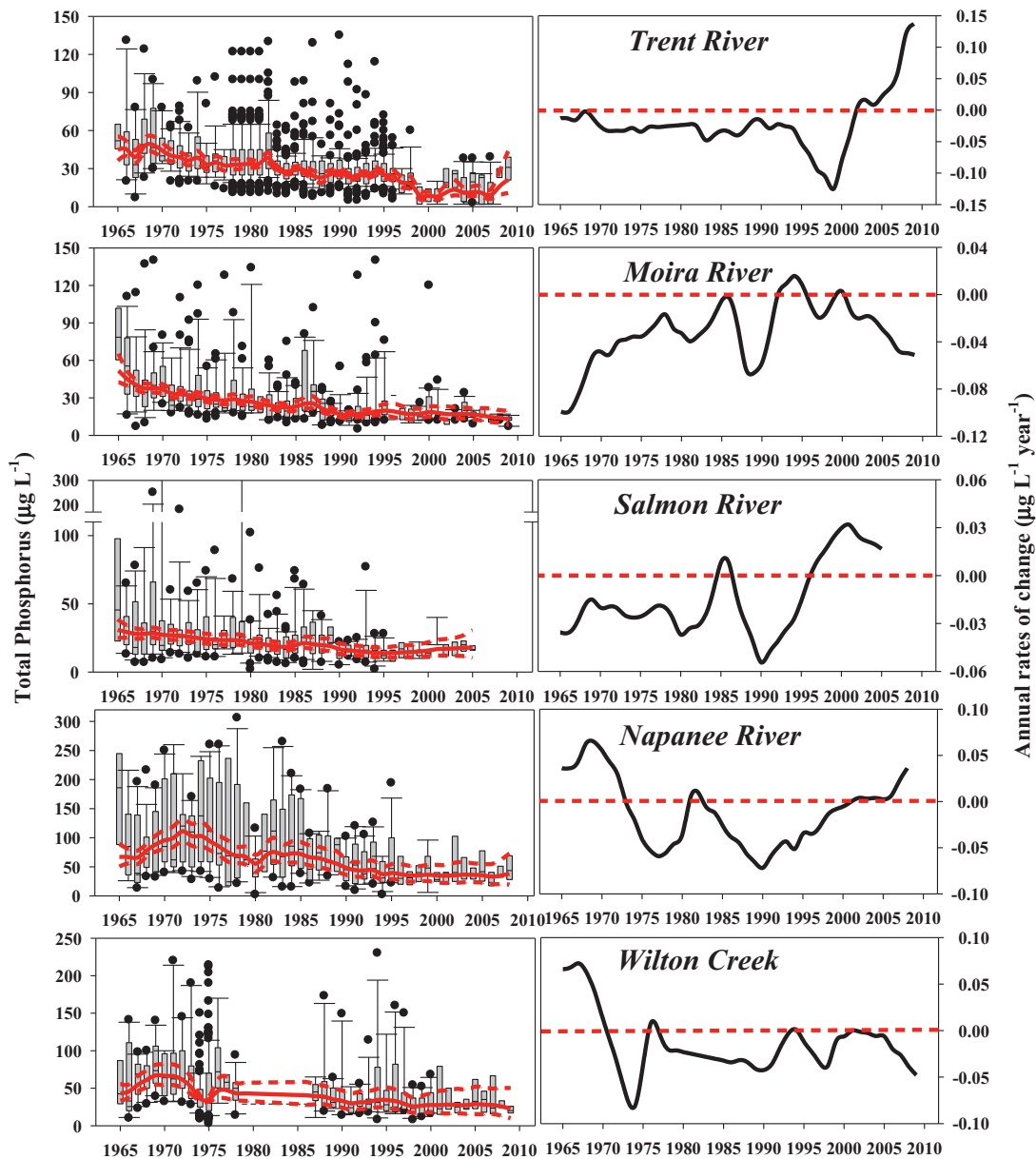
Fig. 3. Dynamic Linear Modeling (*DLM*) analysis of the temporal trends of total phosphorus (*TP*) concentrations in five tributaries of the Bay of Quinte watershed. Left panels depict the mean annual *TP* concentrations when accounting for the covariance with the flow variability (red solid line: mean values, dash lines: 95% posterior predictive intervals, box plots: observed data). Right panels depict the annual rates of change of the log-transformed *TP* concentrations. (For interpretation of the references to color in this figure legend, the reader is referred to the web version of the article.)

the different displacement of phosphorus due to the variability in the corresponding flow regimes induced (Johnson and Owen, 1971). The net loading accommodates the idea that two equal total loads with opposite pairs of flow and concentration, high flow with low concentration or low flow with high concentration, could potentially have a very different effect on the trophic state of the system, and is simply calculated by multiplying the inflows from a particular source with the difference between the inflow and outflow concentrations. During the earlier years of the study period, our analysis showed that the "opposite pair" situation existed in the upper Bay of Quinte, as the computed total seasonal *P* loads would always indicate the river loads were greater, sometimes much more so when river flows were higher. However, the net loading values clearly suggest that the point

sources always made a greater positive contribution, while the river net loads were mostly negative. Net river loads were negative when point source loads were higher, because the point source inputs elevated *TP* concentrations in the system far above the river levels. Hence, when point source loads were high, river inputs actually allowed carrying away some of the excess loading. As both point source loadings and ambient concentrations declined, the river net loads have decreased but still remain negative. The impact of the point-source loading on the prevailing conditions in the Bay of Quinte has been reduced, but it is also important to note that the ambient *TP* concentrations toward the end of summer (August–September) still rise to levels well above the 30 μg L^{-1} target, when the river flows decline to their lowest point.
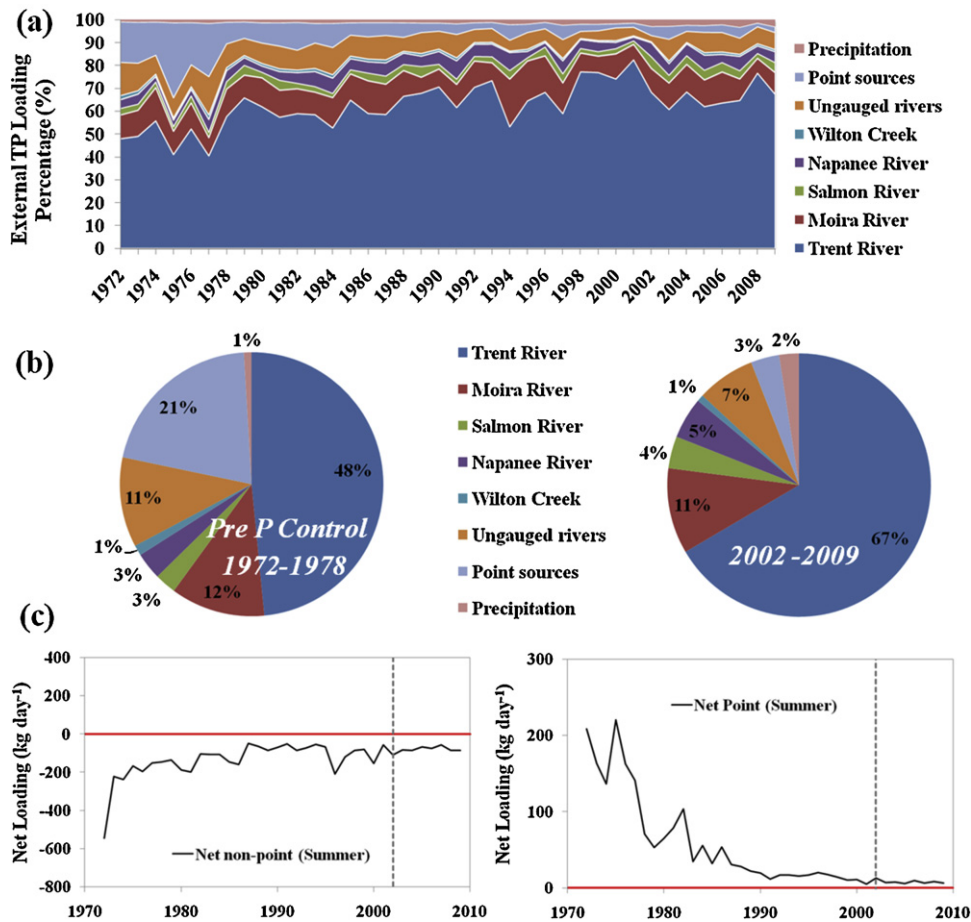
Fig. 4. Temporal trends of exogenous *TP* loading in the Bay of Quinte during the study period (1972–2009): (a) relative contribution from the different loading sources over time; (b) comparison between the pre-control (1972–1978) period (left) and the 2002–2009 period (right); (c) net non-point (left) and point (right) phosphorus loadings into the Upper Bay (=$Flows_{exogenous} \times [TP_{exogenous} - TP_{Upper\ Bay}]$).

3.2. Model performance – sensitivity analysis

The model was calibrated manually to match the observed monthly *TP* patterns in the upper, middle, and lower segments of the Bay during the 2002–2009 period (gray lines in Fig. 5). Because of the significant increase of the model complexity, we had many degrees of freedom to produce virtually any desired behavior. Thus, we opted for a "judicious fiddling" of a subset of the parameter vector (Table 1), while the rest of the parameterization of the macrophyte, dreissenid, and sediment submodels was largely based on their original presentations in the literature (Wang et al., 2003a,b). To understand the functionality of the new *TP* model and put some of the findings of the present analysis into perspective, we subsequently evaluated the influence of different assumptions related to our calibration exercise on the predictive statements made by the model. Goodness-of-fit statistics reflect the satisfactory ability of the model to fit the monthly *TP* levels in the Bay of Quinte (Table 2).

Table 2
Model fit against the observed *TP* concentrations during the 2002–2009 period.

	U_2	U_3	M_1	L_e
AE	3.37	6.50	−4.23	−1.07
r^2	0.52	0.59	0.51	0.00
RMSE	9.71	10.31	10.35	3.50
MEF	0.43	0.13	0.29	−0.43
RE	23%	30%	26%	23%

AE, average error; r^2, determinant coefficient; *RMSE*, root mean squared error; *MEF*, model of efficiency; *RE*, relative error.

In particular, we were able to reproduce the aforementioned end-of-summer increase of the ambient *TP* levels in the upper segment, even in years (e.g., 2005) when the corresponding concentrations were greater than 60 μg L^{-1}. The model also faithfully depicted the spatial gradients in the system, with distinctly higher *TP* levels in the upper segment relative to those experienced in the middle/lower Bay. Notably, the application of the model was characterized by relatively higher R^2 (>0.50), lower *RE* (<30%), and positive *ME* (>0.13) values in the upper and middle segments relative to the corresponding fit statistics in the lower segment. The inferior performance of the model in the epilimnion of the lower segment and its limited capacity to reproduce the late summer-early fall *TP* peaks is closely associated with the assumptions made regarding the dilution effects of the inflows from Lake Ontario (Minns and Moore, 2004; Zhang et al., 2013). For illustration purposes, when this term is switched off during the 2005–2008 period, the underestimation bias is effectively resolved throughout the middle–lower areas (M_1 and L_e) of the system (black dashed lines in Fig. 5).

3.2.1. Macrophyte submodel

Under the assumption that the phosphorus content in macrophyte biomass is 0.0025 g P g dry weight^{-1}, the model outputs fall within the observed range of macrophyte abundance reported by Seifried et al. (2002), 50–150 g dry biomass m^{-2}, with distinctly increasing trends as we move downstream in the Bay (Leisti et al., 2006). The examination of the sensitivity of the *TP* predictions on the characterization of macrophytes in the model primarily highlights the influence of the illumination of the water column on
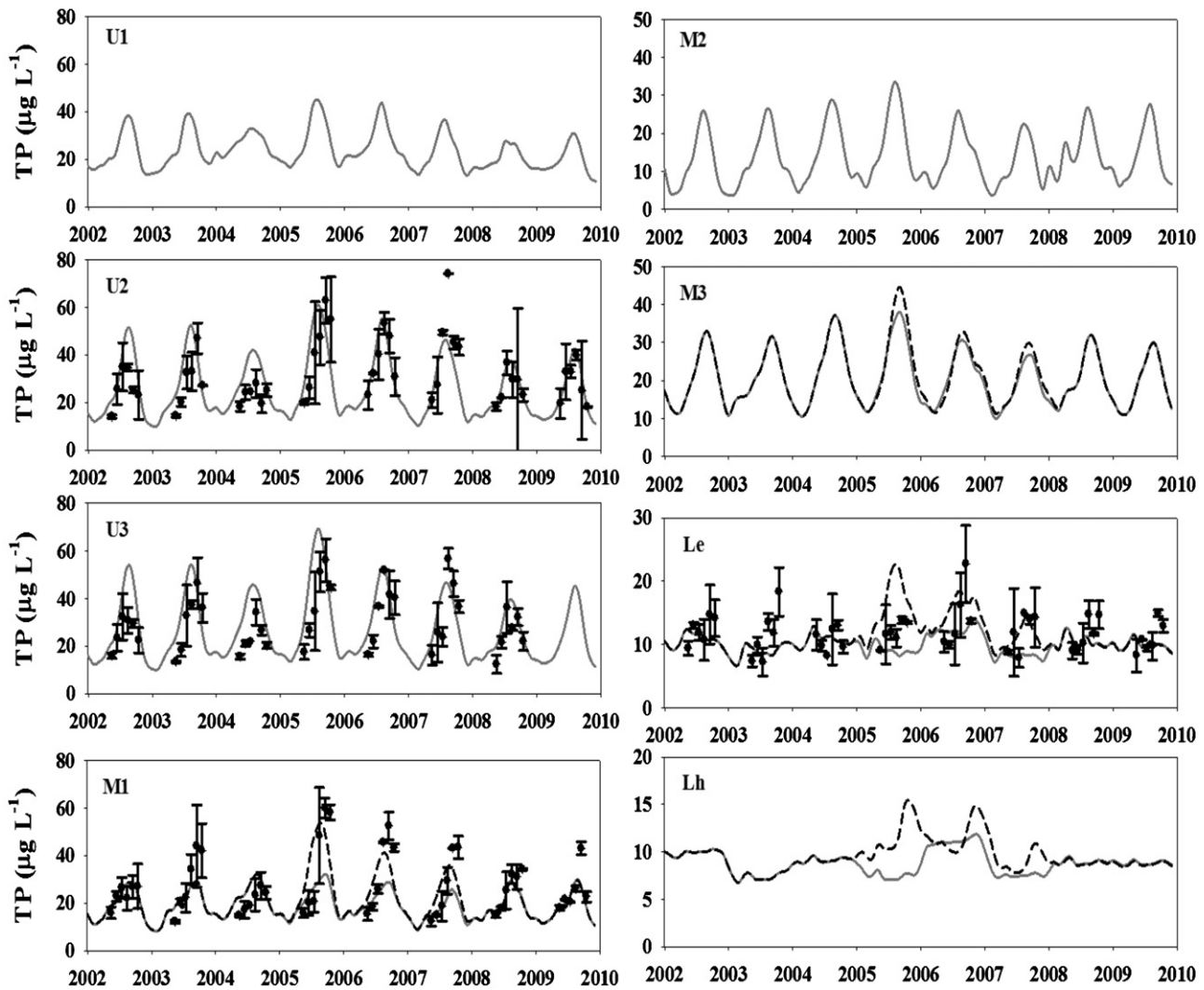
Fig. 5. Simulated versus observed *TP* concentrations in the eight segments of the Bay of Quinte model. Solid lines correspond to the reference model predictions, while dashed lines depict model predictions without backflow interactions.

the ambient *TP* variability, when forcing the model with scenarios of low or high light availability (Fig. SI-1). This pattern predominantly stems from our model assumption that macrophytes directly release phosphorus into the water column through their metabolic by-products. The excessively high *TP* concentrations induced by the scenario of increased water clarity can be controlled by assigning a higher optimal solar radiation for macrophyte growth. By contrast, the parameterization of their affinity for phosphorus does not appear to be an influential factor, as the phosphorus content in the sediment porewater lies well above the growth saturation levels (Fig. SI-2). Another critical facet of this submodel was the sensitivity of *TP* predictions on the phosphorus recycling regimes mediated by macrophytes. Namely, our analysis suggests that the characterization of the macrophyte community as r strategists (i.e., faster growth and metabolic rates) coupled with fast sediment decomposition rates can be an effective calibration strategy for simulating the summer *TP* accumulation in the Bay of Quinte (Fig. SI-3).

3.2.2. Dreissenid submodel

Aside from the absence of different cohort classes, another distinct difference between our dreissenid submodel application and earlier work by Bierman et al. (2005) is that the corresponding differential equation calculates the rate of change of areal dreissenid biomass and not the biomass per individual. Thus, the interannual variability within each segment can be accommodated by the areal colonization rather than the number of mussels per unit area. While it is not clear which of the two variables may be the most reliable proxy of the temporal variability, our experience has been that the use of a constant areal colonization profoundly understates the year-to-year fluctuations of the dreissenid population. We also found that assigning the same parameterization throughout the system cannot simultaneously match the dreissenid biomass levels in both upstream and downstream areas, resulting in a consistent underestimation in the latter segments. While this problem may reflect the transition from a zebra mussel-dominated upper Bay to a quagga mussel-dominated lower Bay (Dermott and Bonnell, 2011), we note that it was overcome by a lower segment-specific dreissenid characterization that postulates more efficient feeding habits (i.e., lower minimum fraction of food egested) along with lower dependence on food availability (Fig. 6; see also Table 1). Finally, the assumptions related to the level of areal colonization (Fig. SI-4) as well as the phosphorus recycling regimes mediated by dreissenids are two critical factors that can determine the *TP* predictions. In particular, a parameterization that postulates fast dreissenid ingestion and respiration rates combined with fast sediment decomposition rates can closely reproduce the end-of-summer *TP* accumulation in the upper Bay (Fig. SI-5).
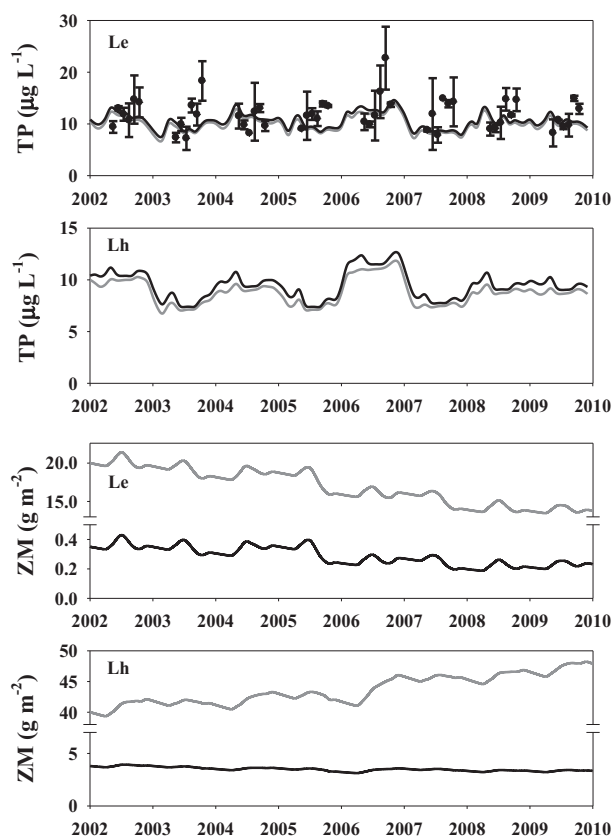
Fig. 6. Model sensitivity to different characterizations of the feeding efficiency of dreissenids (*ZM*) in the lower segment. Black lines correspond to the parameterization that postulates effective dreissenid feeding with low egestion rates and low dependence on food availability. Gray lines depict the assumption that dreissenids are sloppy feeders with high egestion rates and high dependence on food availability.

3.2.3. Sediment submodel

According to the model, the *TP* concentrations in the sediments are ranging from 1.2 to 2.0 mg *TP* g^{-1} dry weight; a prediction that is on par with existing empirical evidence in the system (Environment Canada, unpublished data). Yet, because we lack information about the levels of the individual constituents of the sediment *TP* concentrations (*DIP*, *PIP*, and *OP*), we caution that the good agreement with the observed data may be the result of a series of errors (i.e., misrepresentation of the three state variables) that cancel each other out when they are summed up to calculate the total phosphorus content. Among the parameters used to reproduce the fate and vertical transport of phosphorus in the sediments, we highlight the sensitivity of the ambient *TP* predictions on the values assigned to the sediment porosity. In particular, low sediment porosity is associated with higher *DIP* concentrations, accelerated vertical diffusive exchanges, and therefore higher *TP* concentrations in the water column; especially toward the end of summer-early fall (Fig. SI-6). Similar patterns can be induced from a parameterization that postulates high diffusivity with thicker sediments (Fig. SI-7) as well as predominance of desorption fluxes (Fig. SI-8).

3.3. Evaluation of the role of exogenous loading relative to internal nutrient recycling

Spatial variability of the various external and internal *TP* flux rates in the Bay of Quinte are presented in Fig. 7 and Table 3. The net *TP* contributions (sources or sinks) represent the mass of phosphorus associated with the various compartments (water column, sediments, macrophytes, dreissenids) throughout the growing season (May–October) averaged over the 2002–2009 period. In the U_1 segment, the phosphorus budget is predominantly driven by the external sources (phosphorus loading: 177.4 kg day^{-1}) and sinks (outflows: 209 kg day^{-1}). Interestingly, our model suggests that the sediments (resuspension and diffusion from the sediments to water column minus particle settling) act as a net source of phosphorus in this segment (64.1 kg day^{-1}). Dreissenids approximately subtract 37.6 kg day^{-1} from the water column (particle filtration minus respiration) and subsequently deposit 35.1 kg day^{-1} via their excretion and particle rejection. Likewise, the U_2 segment receives 254.8 kg day^{-1} from exogenous sources, including the upstream inflows, and transports downstream 305.7 kg day^{-1}. The net contribution of the sediments accounts for 103.1 kg day^{-1}, while dreissenids on average reduce the ambient *TP* levels by 93.3 kg day^{-1}. The main difference between the two segments in the upper Bay are the *TP* fluxes related to macrophyte respiration that can reach the level of 72 kg day^{-1}. In a similar manner, the macrophyte intake from the sediments minus the amount of P regenerated from the decomposition of the dead plant tissues can be greater than 40 kg day^{-1} in segments U_3 and M_1, while the subsequent release of their metabolic by-products is approximately responsible for 45–50 kg day^{-1}. Notably, the settling of particulate P dominates over the resuspension and diffusion from the sediments to the water column with the corresponding net fluxes ranging between 25 and 35 kg day^{-1}. In Hay Bay (M_2), the fluxes mediated by the macrophytes and dreissenids primarily modulate the *TP* dynamics and the same pattern appears to hold true in Picton Bay (M_3). In the lower Bay of Quinte (L_e and L_h), the model postulates a significant pathway (>1100 kg P day^{-1}) through which the inflowing water masses from Lake Ontario upwell from the hypolimnion to the epilimnion and are subsequently exported from the system. In the same area, the internal biotic sources (macrophytes and dreissenids) similarly represent an important vector of phosphorus transport.

Table 3
Estimation of *TP* flux rates from different components of the *TP* model.

Site	Net *TP* flux (kg day^{-1})							
	Water–sed	Water–mac	Water–ZM	Sed–ZM	Sed–mac	Burial	Water in	Water out
U_1	64.1	16.4	−37.6	35.0	−13.8	7.3	177.4	209.0
U_2	103.1	71.8	−93.3	86.5	−60.3	16.6	254.8	305.7
U_3	−25.9	46.7	−5.9	5.3	−39.4	3.3	323.3	332.8
M_1	−35.1	49.4	−16.3	15.7	−42.6	2.6	429.4	421.6
M_2	−23.3	50.0	−22.6	21.4	−43.2	2.2	4.2	3.2
M_3	−8.3	12.2	−0.7	0.7	−10.5	0.6	17.3	17.7
L_e	−55.7	45.1	−13.7	13.7	−40.4	3.4	1509.3	1527.6
L_h	24.2	0.0	−62.2	60.7	0.0	8.4	1135.6	1097.3

Water–sed, (resuspension and diffusion from the sediments to water column) – (particle settling); water–mac, (macrophyte respiration); water–ZM, (respiration and 0.4 × excretion of dreissenids) – (particle filtration of dreissenids); sed–ZM, 0.6 × excretion, egestion and rejection from dreissenids; sed–mac, (macrophyte mortality) – (macrophyte intake from sediment); burial, burial rate into deeper layers; water in, upstream inflow and external loading; water out, downstream outflow.
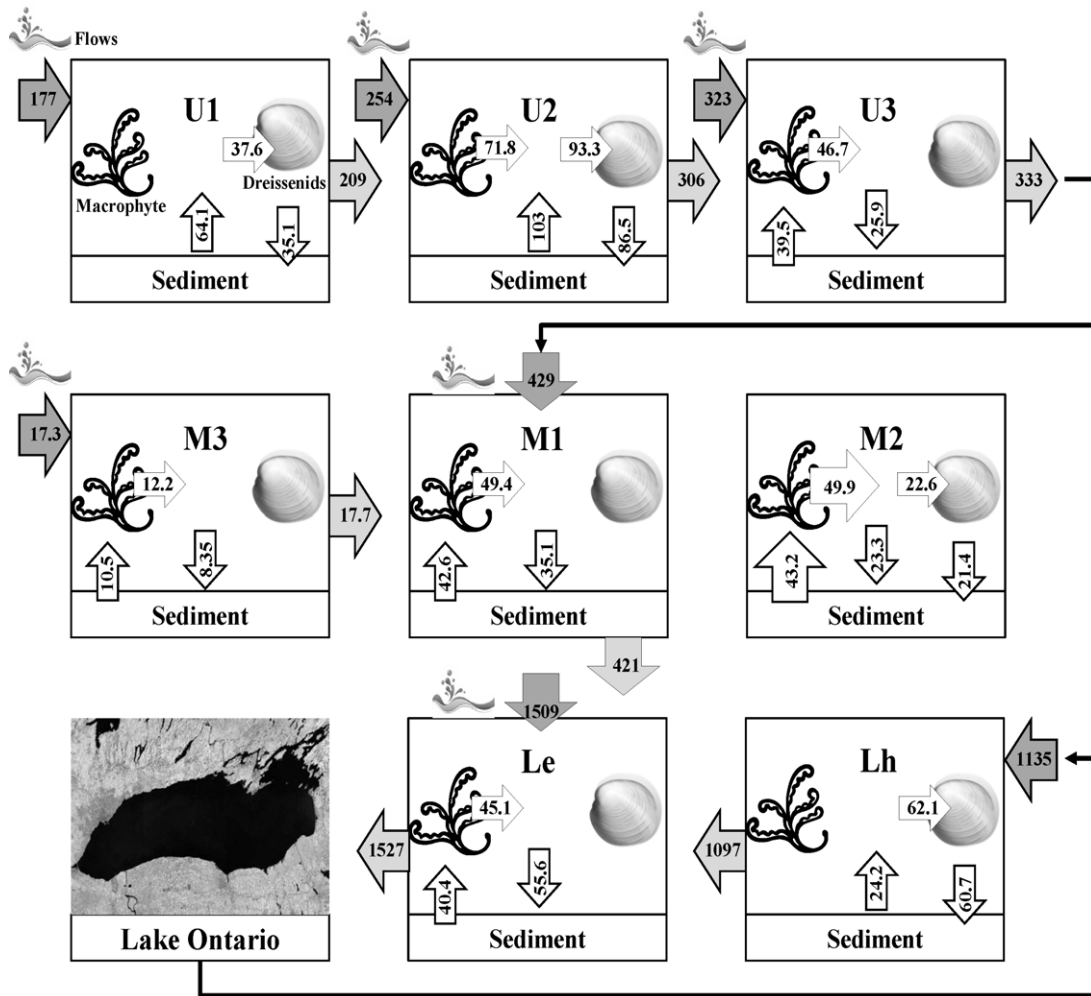
Fig. 7. Spatial variability of the various external and internal *TP* flux rates in the Bay of Quinte. Arrow directions indicate the net contribution (sources or sinks) of the various compartments (water column, sediments, macrophytes, dreissenids). Gray arrows show the *TP* inflows in a spatial segment, while the light-blue ones depict the corresponding outflows.

The effects of submerged aquatic macrophytes on the ambient nutrient concentrations through the production/processing of organic matter and nutrient cycling have received a fair amount of attention in the literature (Barko and James, 1998; Bini et al., 2010; Christensen, 1999; Eriksson and Weisner, 1999; Sand-Jensen, 1998; Wigand et al., 1997; Zimmer et al., 2001). Several mechanisms may determine the role of aquatic macrophytes as either nutrient sources or sinks in the surrounding water (Petticrew and Kalff, 1992). Generally, the submerged macrophytes could provide a major pathway for the rapid transport of the nutrients assimilated from the sediments into the water column; a process known as "nutrient pump effect" (Asaeda et al., 2000; Howard-Williams and Allanson, 1981). Further, the decomposition of dead plant tissues may be an important source of nutrients, especially since macrophytes demonstrate high capacity of luxury uptake and thus tend to accumulate nutrients in concentrations higher than their physiological requirements (Bini et al., 2010). Productive macrophyte stands could also cause hypoxia at night-time, thereby accelerating *P* release from the sediments (Bini et al., 2010). Even in oxygenated water though, the increased photosynthetic rates elevate water pH (ca. 9–10), which in turn similarly increases the sediment *P* fluxes (Barko and James, 1998). On the other hand, there is another suite of mechanisms that can potentially counterbalance the release of phosphorus from the macrophyte metabolic activity, such as foliar absorption or rapid phytoplankton uptake (Rørslett et al., 1986),

and thus their presence may not always be positively related to the ambient nutrient concentrations. Importantly, our model does include the "nutrient pump effect", but does not explicitly account for pathways that could offset the macrophyte phosphorus release into the water column. Hence, the present modeling structure (and the resulting parameterization) may place more weight on the role of macrophytes at the expense of other potentially important internal nutrient sources in the system, e.g., diffusive exchange in the sediment–water column interface.

In the Bay of Quinte, the controlling factors of the submerged macrophyte distribution and abundance are the depth, the water transparency, the fetch/wave exposure, the sediment texture and stability (Leisti et al., 2006; Seifried, 2002). Significant increases in macrophyte cover were recorded throughout the system after the invasion of zebra mussels, and existing empirical evidence indicates that higher densities were first established in the shallower areas and gradually proliferated into deeper waters with increasing water clarity (Seifried, 2002). To consolidate our previous findings on the relative importance of internal loading, we further evaluated the changes of the *TP* flux rates under the nutrient recycling regimes mediated by distinctly different specifications of the simulated macrophyte community (Table 4). In particular, depending on the macrophyte characterization as r or K strategists (i.e., organisms with faster/slower maximum growth and metabolic rates) in conjunction with a parameterization that

Table 4

Relative changes of the TP flux rates under fast and slow recycling regimes, mediated by macrophytes and dreissenids. Abbreviations are provided in the footnote of Table 3.

	Site	ΔTP flux (kg day^{-1})							
		Water–sed	Water–mac	Water–ZM	Sed–ZM	Sed–mac	Burial	Water in	Water out
Mac	U_1	9.05	30.59	−13.94	12.85	−26.47	−0.07	0.00	24.86
	U_2	−33.98	133.39	−41.74	38.02	−115.45	−0.19	24.86	76.91
	U_3	−21.28	75.15	−4.75	4.25	−65.14	−0.16	76.91	123.17
	M_1	−15.75	55.90	−17.68	16.75	−49.18	−0.11	147.58	166.83
	M_2	−17.81	59.78	−39.51	36.79	−52.89	−0.02	0.00	1.93
	M_3	−5.54	13.39	−1.49	1.37	−11.81	−0.02	7.15	11.02
	L_e	−3.26	40.15	−0.09	0.07	−35.89	−0.22	190.46	228.74
	L_h	18.75	0.00	−0.29	0.26	0.00	−0.10	0.00	30.79
ZM	U_1	29.93	0.41	−20.09	18.23	−0.37	−0.02	0.00	9.78
	U_2	60.18	1.93	−26.96	23.55	−1.74	−0.08	9.78	38.33
	U_3	−2.27	2.20	−1.88	1.57	−2.01	0.00	38.33	34.84
	M_1	−3.18	12.56	−11.99	11.40	−11.43	0.02	40.33	35.43
	M_2	−1.42	9.87	−8.17	7.55	−8.98	0.00	0.00	0.13
	M_3	−1.07	3.16	−0.56	0.51	−2.87	0.00	1.38	2.18
	L_e	−0.56	19.49	−0.07	0.06	−18.69	−0.08	53.25	70.98
	L_h	17.69	0.00	−1.82	1.69	0.00	−0.08	0.00	19.19

ΔTP flux = TP fluxes with fast P recycling − TP fluxes with slow P recycling.

postulates fast or slow sediment decomposition rates, the macrophyte intake from the sediments minus the amount of P regenerated from the decomposition of the dead plant tissues can vary between 25 and 115 kg day^{-1} in the different segments of the upper Bay, while the subsequent P release through their metabolism may approximately range between 30 and 135 kg day^{-1}. The same trend is also manifested in the main stem of the middle and lower Bay, where the net contribution of the macrophyte pathways that act as phosphorus sources in the water column or as sinks in the sediments can vary between 40–55 kg day^{-1} and 35–50 kg day^{-1}, respectively. In Hay Bay (M_2), the macrophyte processes appear to exert control on the P budget (>50 kg day^{-1}). Interestingly, our analysis also reveals a co-dependence between macrophyte and dreissenid activity in the same area (underlined numbers in Table 4), suggesting that the magnitude of the macrophyte "nutrient pump effect" can potentially induce considerable variations in the amount of particles filtered/ingested by the dreissenids as well as in their excretion/pseudofeces production rates (Vanderploeg et al., 2001). Given that the corresponding exogenous subsidies are fairly low (see details of their derivation in the companion paper by Zhang et al., 2013), the latter finding indirectly reflects a greater reliance of this embayment upon nutrient regeneration processes. Generally, our analysis suggests an increasing dependence of the ecosystem functioning on internal mechanisms as we move toward Lake Ontario, which may be causally related to the spatiotemporal changes of the lower food web structure reported by Munawar et al. (2011). Namely, the lower food web appears to undergo periodic structural shifts between autotrophs and heterotrophs in the upper segments, whereas the microbial loop components consistently represent the greatest proportion of the organic carbon pool in the lower Bay (Munawar et al., 2011).

A similar exercise with the nutrient recycling regimes mediated by the dreissenids primarily highlighted their relative importance in the P budget of the upper Bay, although the variability induced was significantly lower than the values found from our previous experiment with the macrophytes (Table 4). As previously mentioned, the dreissenid submodel in its present form requires a user-specified areal colonization, and therefore lacks the ability to predict changes in spatiotemporal densities or the distributions of dreissenids among different age groups. Because our experience has been that the assumption of a constant areal colonization underestimates the observed year-to-year biomass variability (Dermott and Bonnell, 2011), the development of a population dynamics model that will explicitly consider the factors

that predominantly drive the dreissenid temporal patterns (e.g., round goby) in the system is certainly the way forward (Bowen and Johannsson, 2011).

3.4. Analysis of nutrient loading scenarios

While the intermediate to deeper depths in the Bay of Quinte minimize the likelihood of alternate stable states to occur (Seifried, 2002), the sizable contribution of nutrient loading from internal sources underscores the challenges associated with the determination of critical exogenous nutrient loads for achieving the delisting TP criterion of 30 µg L^{-1}. In this regard, we first examined the nature of the relationship between the riverine TP concentrations and the ambient TP levels at the upper segments of the Bay of Quinte, as manifested in the post-dreissenid period. In our numerical experiments, the first eight years of each simulation were based on the actual meteorological and loading forcing during the 2002–2009 period, while the final (ninth) year was forced with the external conditions of one of the last fourteen years (1996–2009). The same experiments were repeated by assuming a 40% reduction of the river TP concentrations during the final simulated year. In addition to the complex model, we also used the PM_{2012} version of the Minns and Moore (2004) model, as modified by Zhang et al. (2013), to assess the range of dynamics that can be reproduced by the two modeling constructs. The greater amplitude of the complex model simulations are indicative of its sensitivity to external perturbations and therefore its capacity to more sensibly depict the induced changes in the intra-annual TP variability (Fig. 8a–d). We then used the complex model outputs for the final year to examine the relationship between flow-weighted TP input concentrations from non-point sources and the seasonal ambient TP in the Upper Bay (Fig. 8e). Our results suggest that the seasonal average TP concentrations consistently exceed the value of 30 µg L^{-1} within the currently experienced riverine concentration range. However, a decrease of the TP inflows from the local tributaries is likely to bring about distinct water quality improvements, although there will still be protracted periods when the targeted TP level is exceeded (Fig. 8f). The innermost area of the Bay (segment U_1), directly influenced by the Trent River discharges, is particularly responsive to the variations of the non-point nutrient inflows, but the impact of the loading reductions is gradually lessened as we move downstream.

Even though the projected limited system response to the nutrient loading scenarios examined certainly adds an element of skepticism about the future management actions in the area,
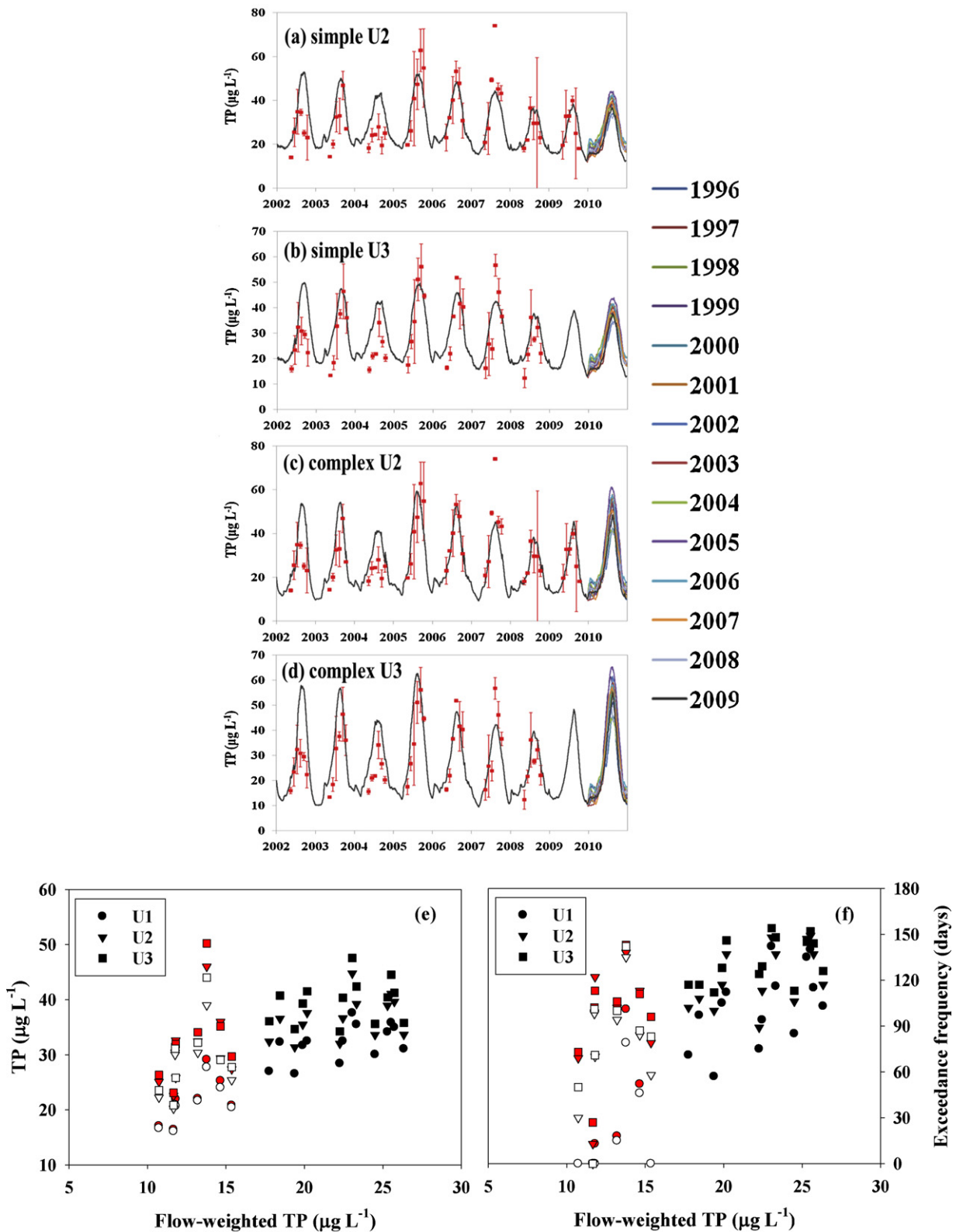
Fig. 8. Simulated *TP* concentrations at the upper segments of the Bay of Quinte. The first eight years of each simulation are based on the actual meteorological and loading forcing during the 2002–2009 period, while the final (ninth) year is forced with the external conditions of one of the last fourteen years (1996–2009). The simple (a and b) and complex (c and d) model predictions of the fourteen simulated scenarios at the U_2 and U_3 segments; (e) relationship between flow-weighted *TP* input concentrations from non-point sources and predicted seasonal ambient *TP* in the Upper Bay; and (f) relationship between flow-weighted *TP* concentrations and the days when the delisting criterion of 30 μg L^{-1} is exceeded. Black dots correspond to projected *TP* concentrations under current exogenous loading conditions. Gray dots correspond to predicted *TP* concentrations in response to 40% exogenous loading reduction. White dots indicate predicted *TP* concentrations in response to 40% of exogenous loading reduction along with an adaptive increase of the feeding efficiency of dreissenids.

our projections should be viewed with caution for two basic reasons. First, our analysis is strictly deterministic in that our model projections are entirely based on the ecological structure postulated by the calibration vector. In doing so, we fail to consider the "*known or unknown ecological unknowns*" (sensu Gudimov et al., 2011), such as the broader range of adaptive mechanisms and non-linearities of ecological behaviors that can potentially modulate the system response and therefore shape its restoration pace. For example, if we assume an adaptive increase of the dreissenid feeding efficiency following the reduction of exogenous loading and the subsequent decrease in the suspended particles in the water column, the predicted *TP* concentrations can be further diminished by 2–5 μg L^{-1} (Fig. 8e and f). Second, all the predictions so far are contingent upon the assumptions made regarding the contemporary nutrient loading, and thus the likelihood of a systematic underestimation due to the lack of reliable urban runoff estimates or the inconsistent event-based sampling is not explicitly accounted for (Kinstler and Morley, 2011; XCG Consultants Ltd., 2009; Zhang et al., 2013). The latter point suggests that our model parameterization may offset the underestimation bias in the exogenous loading by unnecessarily overstating the importance of the internal nutrient fluxes. To examine the robustness of the previous model projections, we hypothesized that the current estimates underestimate by half the actual *TP* loading during the 2002–2009 period. The model was recalibrated to match the observed data by downplaying the importance of the nutrient subsidies from dreissenids, macrophytes, and sediment diagenesis (see alternative parameterization in Table 1). Following the previously described design, we conducted experiments in which the model was forced with a wide range of combinations of *TP* riverine concentrations and flows, and the point loading was set equal to the lowest annual level (7.0 kg day^{-1}) reported during the 2002–2009 period. Our analysis paints a more favorable picture relative to the scenarios that assume error-free loading estimates. Namely, the predicted maximum monthly *TP* concentrations in the upper Bay were lower than 30–35 μg L^{-1} across a wide range of flow conditions, when the flow-weighted *TP* concentration approximately falls below the level of 20 μg L^{-1}. Interestingly, our simulations also suggest that the maximum monthly ambient *TP* levels will be further reduced by 5–15% (or 1–3 μg L^{-1}), if the same reduced loading conditions prevail for about 5–10 years (Fig. SI-9).

4. Synthesis – next steps

In this series of two papers, we presented an analysis that primarily aimed to indicate the optimal modeling construct for guiding the eutrophication management decisions in the Bay of Quinte, Ontario, Canada. The first objective was to examine the capacity of a simple *TP* mass-balance model, originally developed by Minns and Moore (2004), to accurately reproduce the spatiotemporal phosphorus dynamics in the system. Generally, our viewpoint has been that there are several compelling reasons to adopt simplicity in the contemporary modeling practices; especially, when the model is intended to offer first-order approximations of the ecosystem functioning. Simple models can be understood more easily, have fewer unconstrained parameters, and are subjected more easily to detailed sensitivity analyses (Arhonditsis and Brett, 2004). Hence, our main criticism of the existing *TP* model does not stem from its simplicity per se, but rather from its structural inadequacy to represent one of the most critical facets of the eutrophication problems in the area, i.e., the causal association among exogenous loading, internal recycling, and end-of-summer ambient concentrations. Our analysis provided evidence that the Minns and Moore (2004) model can reliably support predictive statements only on a seasonal scale (e.g., summer *TP* averages), and cannot capture the full range of daily *TP* concentrations typically experienced in

the Bay of Quinte; even when temperature-dependent sediment reflux rates along with a refined spatial resolution are considered (Zhang et al., 2013; e.g., see simulated patterns in Fig. 3). It is abundantly clear that we need to invoke extra complexity for impartially studying the complex interplay among macrophytes, dreissenids, and sediment diagenesis that appears to modulate the nutrient recycling in the present state of the Bay.

In this regard, the increased articulation level of the present model undoubtedly offers greater flexibility in reproducing the broad range of *TP* dynamics in the system (Fig. 8). Although not formally calibrated with optimization or Bayesian inference techniques, the model agreement with the observed *TP* patterns has significantly improved and our sensitivity analysis identified several distinctly different parameterization strategies that can conceivably explain the end-of-summer/early fall *TP* accumulation. Yet, the improved performance of a complex overparameterized model is neither surprising nor guarantees the credibility of the projected system trajectories under alternative management schemes (Arhonditsis et al., 2006, 2007; Reichert and Omlin, 1997). Rather, the inflated parametric and structural uncertainty increases the likelihood to obtain "good results for the wrong reasons", thereby undermining any efforts to tease out definitive conclusions or predictive statements from the model (Arhonditsis and Brett, 2004). When viewed in this context, the primary value of the present model construct was its ability to offer testable hypotheses and mechanistic insights into the phosphorus cycling in the system.

According to our modeling analysis, Trent River is the predominant driver of the upper Bay dynamics until the main stem of the middle area (Zhang et al., 2013). Similar to earlier assertions though (Minns et al., 2004), we also found that the sediments in the same area act as a net source of phosphorus and the corresponding fluxes are likely magnified by the macrophyte and dreissenid activity, e.g., nutrient pump effect and pseudofeces production. From a management standpoint, the presence of an important positive feedback loop in the upper Bay suggests that the anticipated benefits by an additional reduction of the exogenous point and non-point loading may not be realized within a reasonable time frame (Gudimov et al., 2011; Scheffer et al., 2001). In fact, our analysis of nutrient loading scenarios provided ample evidence that the restoration pace of the Bay could be very slow, even if the riverine *TP* concentrations reach levels significantly lower than their contemporary values, <20–25 μg *TP* L^{-1}. These ominous forecasts are further complicated by the recently increasing *TP* trends in several local tributaries, although the Trent River concentrations are still lying below the ambient *TP* levels. Given the considerable efforts to reduce both point and non-point loading discharges over the last four decades, our model predictions may seem somewhat disturbing and certainly underscore the challenges in determining the suitable management actions in the area. In our view, the *most critical* research question is the verification (or further refinement) of the existing loading estimates and subsequently the consolidation of their causal association with the prevailing conditions in the historical monitoring sites. In this study, we showed that the likelihood of an underestimation bias in the exogenous loading used to force the model may have led to a situation, in which two errors (underestimation of the exogenous and overestimation of the internal loading) canceled each other out and resulted in a misleadingly satisfactory model fit. If this hypothesis holds true, then our model parameterization overstates the strength of nutrient recycling, and thus the response of the system could actually be faster than the original projections (Fig. 9).

One of the basic requirements for establishing sensible delisting objectives is the identification of a *TP* numerical value that is both scientifically sound and attainable (Zhang et al., 2013). In regards to the achievability, our modeling analysis was somewhat inconclusive, as all our predictive statements were contingent upon
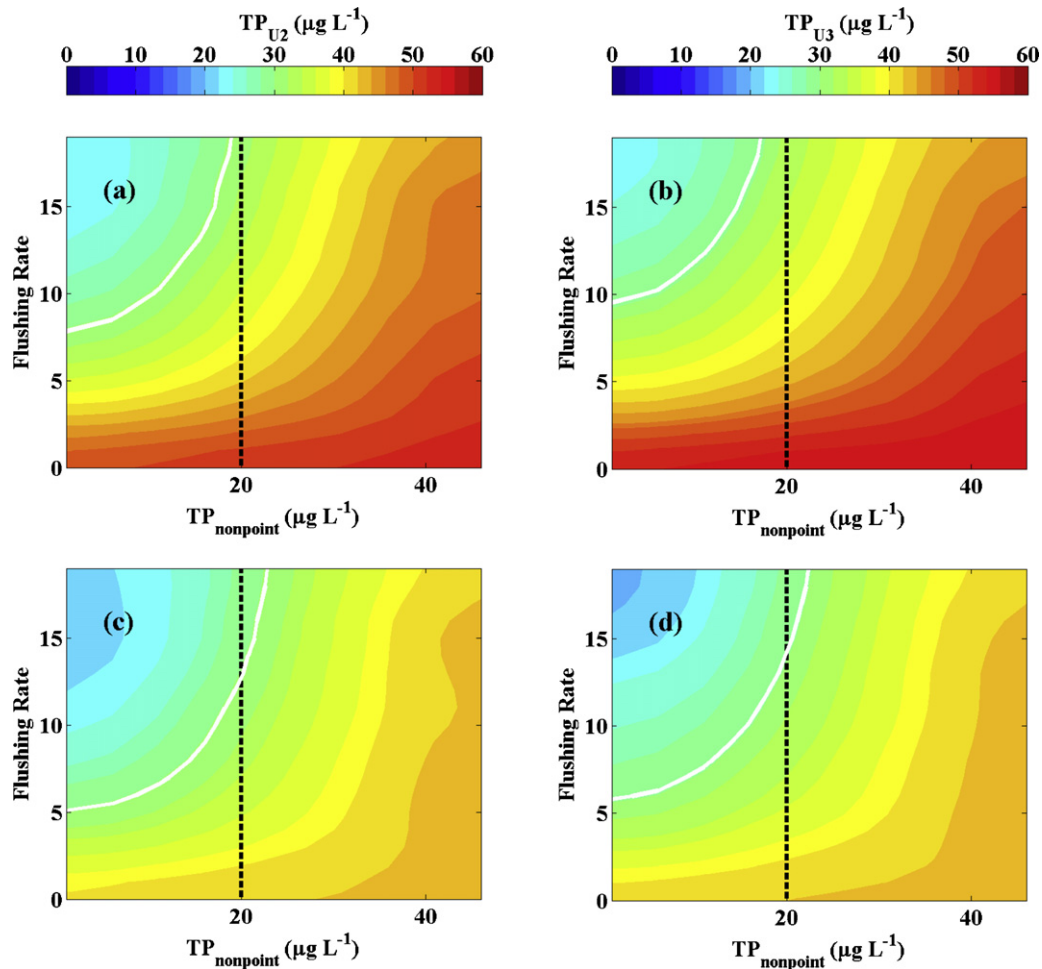
Fig. 9. Simulated maximum monthly *TP* concentrations during the growing season (May–October) in the Bay of Quinte. *Upper panels* refer to the predictions associated with the reference environmental conditions; and *lower panels* represent the predictions of the same model, recalibrated with twofold increase of the external loading forcing. The first eight years (2002–2009) of each simulation were based on real meteorological and loading forcing, while the final (ninth) year was forced with a wide range of combinations of *TP* riverine concentrations and flows. These experiments were conducted with the point loading set equal to the lowest summer seasonal level (7.0 kg day^{-1}) reported during the 2002–2009 period. The white contour line corresponds to the currently targeted seasonal level of 30 μg *TP* L^{-1}. The flushing rates express the frequency (number of times) of water renewal in the upper Bay during the growing season. [The subscript U_2 refers to the segment that begins from the mouth of Moira River and comprises the Big Bay, Muscote Bay, and North Point Bay; and U_3 represent the area influenced by the inflows of Napanee River, extending until the outlet of Hay Bay.]

the prevailing hydrodynamic conditions and the credibility of the current nutrient loading estimates. However, these equivocal projections should not be perceived as evidence in support of the present "status quo" in the Bay of Quinte, but rather a reinforcement of the pragmatic standpoint that criteria should explicitly accommodate all the sources of uncertainty, such as insufficient information, lack of knowledge, natural variability, unaccounted "ecological unknowns", by adopting a probabilistic approach that permits a realistic frequency of violations, e.g., when the targeted water quality goal is violated 10% or less in space and time, the system should still be considered as non-impaired (Office of Water, 1997; Ramin et al., 2011; Reckhow et al., 2005). The next critical step evaluates the appropriate spatiotemporal resolution upon which management decisions can be based. In our companion paper (Zhang et al., 2013), we argued against the currently targeted seasonal average *TP* concentration of 30 μg L^{-1} monitored in a couple of offshore sites of the upper Bay, asserting that is neither a reflection of the actual temporal variability in the system nor representative of the water quality conditions in areas of high public exposure (e.g., beaches). Given the considerable intra-annual variability during the May to October period or the significant spatial heterogeneity between nearshore and offshore sites, it is very unlikely that a single-valued water quality standard can faithfully

depict the entire range of dynamics in the system or the magnitude of the end-of-summer *TP* peaks.

One point of clarification is that the adoption of a probabilistic approach to nutrient criteria is not a means of making P targets more or less attainable, but rather it offers a more comprehensive method to track the prevailing conditions in the Bay. For example, if we the assume that the *TP* concentrations in the Bay of Quinte follow a log-normal distribution and that *TP* values <15 μg L^{-1} are likely to occur only 10% of the time during the growing season, then an average value of 30 μg *TP* L^{-1} implies that we also accept 10% exceedances of the 50 μg *TP* L^{-1} level. According to the mean predictions of the regression models presented by Zhang et al. (2013), the latter likelihood approximately translates into a 10% probability of exceeding 25 μg L^{-1} chlorophyll *a*. If we also consider the recently reported weak correlation between chlorophyll *a* and cyanobacterial toxin concentrations in this embayment (Watson et al., 2011), then it can be easily inferred that the uncertainty in the overall assessment of the Beneficial Use Impairment "*Eutrophication and Undesirable Algae*" can be considerably inflated by any misspecification in the *TP* criterion. Bearing in mind that the *TP* target merely represents a "means to an end" and not "the end itself", the actual question that the local stakeholders should ponder is to what extent these violations represent acceptable risks that

they are willing to take while still classifying the system as non-impaired? It is also our belief that the water quality management can be more meaningfully assisted when the delisting decisions revolve around extreme values, e.g., critical levels of water quality variables that more closely depict undesirable states, rather than acceptable average conditions that will implicitly accommodate the extremes.

Given the above context, we favor the adoption of a *TP* criterion that is focused on extreme states and overcomes the problem of a coarse spatiotemporal resolution. The same water quality goal should be possible to monitor and effectively weigh the dynamics of both nearshore and offshore areas. A tentative critical threshold could be the value of $40 \, \mu g \, TP \, L^{-1}$ which cannot be exceeded more than 10–15% in both time and space. [Notably, if we follow the previous reasoning, this criterion is approximately equivalent to a targeted seasonal average of 25–$28 \, \mu g \, TP \, L^{-1}$.] The compliance formula should be based on both historical monitoring stations (Belleville, Napanee) as well as nearshore sites of public interest in the upper Bay. The sampling frequency must be at least twice a month during the growing season, i.e., from early or mid-May to the end of September. Further, according to our model simulations, the proposed water quality goal is likely to be met, if we approximately achieve a $20 \, \mu g \, TP \, L^{-1}$ flow-weighted concentration from all the major tributaries discharging in the upper Bay in combination with point loadings at the level of $7.0 \, \mathrm{kg} \, \mathrm{day}^{-1}$ (or less) during the growing season.

We conclude by stressing two major issues stakeholders need to consider. The first decision involves the selection of the optimal numerical value to postulate the dichotomy between impaired and non-impaired conditions (Office of Water, 1997; Ramin et al., 2011; Reckhow et al., 2005). The proposed value of $40 \, \mu g \, TP \, L^{-1}$ is on par with the typical values used to delineate the mesotrophic conditions and as such is scientifically defensible (Wetzel, 2001). Yet, it may be desirable to introduce different threshold levels for offshore and nearshore areas, if the use of one single value is deemed to impose a disproportional penalty on nearshore zones or to unjustifiably lower the bar in offshore waters. The second decision is not mutually exclusive with the first one and questions the weights that nearshore and offshore sites are given in the overall assessment of the system. Simply put, if the *TP* variability over the entire system is emulated by a mixture probability distribution, then it is critical to determine the weights assigned to the mixture components, i.e., the relative importance of the constituent density functions that reflect the prevailing conditions in the individual monitoring sites (Gelman et al., 2004). These decisions should effectively balance between environmental concerns and socioeconomic values, thereby reflecting how all citizens, businesses, industries, and the governing councils view the potential of the Bay of Quinte to be a symbol of an environmentally sustainable community.

Appendix A. Supplementary data

Supplementary data associated with this article can be found, in the online version, at http://dx.doi.org/10.1016/j.ecolmodel.2013.02.017.

References

Arhonditsis, G.B., Adams-VanHarn, B.A., Nielsen, L., Stow, C.A., Reckhow, K.H., 2006. Evaluation of the current state of mechanistic aquatic biogeochemical modeling: citation analysis and future perspectives. Environmental Science and Technology 40, 6547–6554.

Arhonditsis, G.B., Brett, M.T., 2004. Evaluation of the current state of mechanistic aquatic biogeochemical modeling. Marine Ecology Progress Series 271, 13–26.

Arhonditsis, G.B., Qian, S.S., Stow, C.A., Lamon, E.C., Reckhow, K.H., 2007. Eutrophication risk assessment using Bayesian calibration of process-based models: application to a mesotrophic lake. Ecological Modeling 208, 215–229.

Asaeda, T., Trung, V.K., Manatunge, J., 2000. Modeling the effects of macrophyte growth and decomposition on the nutrient budget in Shallow Lakes. Aquatic Botany 68, 217–237.

Barko, J.W., James, W.F., 1998. Effects of submerged aquatic macrophytes on nutrient dynamics, sedimentation, and resuspension. In: Jeppesen, E., Søndergaard, M., Christoffersen, K. (Eds.), The Structuring Role of Submerged Macophytes in Lakes. Springer-Verlag, New York, pp. 197–214.

Bierman, V.J., Kaur, J., DePinto, J.V., Feist, T.J., Dilks, D.W., 2005. Modeling the role of zebra mussels in the proliferation of blue-green algae in Saginaw Bay, Lake Huron. Journal of Great Lakes Research 31, 32–55.

Bini, L., Thomaz, S., Carvalho, P., 2010. Limnological effects of *Egeria najas* Planchon (Hydrocharitaceae) in the arms of Itaipu Reservoir (Brazil, Paraguay). Limnology 11, 39–47.

Bowen, K.L., Johannsson, O.E., 2011. Changes in zooplankton biomass in the Bay of Quinte with the arrival of the mussels, *Dreissena polymorpha* and *D. rostiformis bugensis*, and the predatory cladoceran, *Cercopagis pengoi*: 1975 to 2008. Aquatic Ecosystem Health and Management Society 14, 44–55.

Brittain, S.M., Wang, J., Babcock-Jackson, L., Carmichael, W.W., Rinehart, K.L., Culver, D.A., 2000. Isolation and characterization of microcystins, cyclic heptapeptide hepatotoxins from a Lake Erie strain of *Microcystis aeruginosa*. Journal of Great Lakes Research 26, 241–249.

Chao, X., Jia, Y., Shields Jr., F.D., Wang, S.S.Y., Cooper, C.M., 2008. Three-dimensional numerical modeling of cohesive sediment transport and wind wave impact in a shallow oxbow lake. Advances in Water Resources 31, 1004–1014.

Chapra, S.C., 1997. Surface Water-Quality Modeling. McGraw-Hill, New York.

Christensen, K.K., 1999. Comparison of iron and phosphorus mobilization from sediments inhabited by *Littorella uniflora* and *Sphagnum* sp. at different sulfate concentrations. Arch Hydrobiol 145, 257–275.

Coastal Engineering Research Center (CERC), 1994. Shore Protection Manual. U.S. Army Corps of Eng., Washington, D.C.

Coleman, F.C., Williams, S.L., 2002. Overexploiting marine ecosystem engineers: potential consequences for biodiversity. Trends in Ecology and Evolution 17, 40–44.

Congdon, P., 2001. Bayesian Statistical Modelling. John Wiley & Sons Ltd., New York.

Dermott, R., Bonnell, R., 2011. Benthic Fauna in the Bay of Quinte. Kingston, Ontario, Canada.

deYoung, B., Barange, M., Beaugrand, G., Harris, R., Perry, R.I., Scheffer, M., Werner, F., 2008. Regime shifts in marine ecosystems: detection, prediction and management. Trends in Ecology and Evolution 23, 402–409.

Eriksson, P.G., Weisner, S.E.B., 1999. An experimental study on effects of submersed macrophytes on nitrification and denitrification in ammonium-rich aquatic systems. Limnology and Oceanography 44, 1993–1999.

Gelman, A., Carlin, J.B., Stern, H.S., Rubin, D.B., 2004. Bayesian Data Analysis. Champman & Hall/CRC, Boca Raton, FL.

Gudimov, A., Ramin, M., Labencki, T., Wellen, C., Shelar, M., Shimoda, Y., Boyd, D., Arhonditsis, G.B., 2011. Predicting the response of Hamilton Harbour to the nutrient loading reductions: a modeling analysis of the ecological unknowns. Journal of Great Lakes Research 37, 494–506.

Hecky, R.E., Smith, R.E., Barton, D.R., Guildford, S.J., Taylor, W.D., Charlton, M.N., Howell, T., 2004. The nearshore phosphorus shunt: a consequence of ecosystem engineering by dreissenids in the Laurentian Great Lakes. Canadian Journal of Fisheries and Aquatic Sciences 61, 1285–1293.

Holland, R.E., Johengen, T.H., Beeton, A.M., 1995. Trends in nutrient concentrations in Hatchery Bay, western Lake Erie, before and after *Dreissena polymorpha*. Canadian Journal of Fisheries and Aquatic Sciences 52, 1202–1209.

Howard-Williams, C., Allanson, B.R., 1981. Phosphorus cycling in a dense *Potamogeton pectinatus* L. Bed. Oecologia 49, 56–66.

Jacoby, J.M., Collier, D.C., Welch, E.B., Hardy, F.J., Crayton, M., 2000. Environmental factors associated with a toxic bloom of *Microcystis aeruginosa*. Canadian Journal of Fisheries and Aquatic Sciences 57, 231–240.

James, W.F., Barko, J.W., Eakin, H.L., 1997. Nutrient regeneration by the Zebra Mussel (*Dreissena polymorpha*). Journal of Freshwater Ecology 12, 209–216.

Jassby, A.D., Platt, T., 1976. Mathematical formulation of the relationship between photosynthesis and light for phytoplankton. Limnology and Oceanography 21, 540–547.

Johnson, M.G., Owen, G.E., 1971. Nutrients and nutrient budgets in the Bay of Quinte, Lake Ontario. Journal WPCF 43, 836–853.

Kinstler, P., Morley, A., 2011. Point Source Phosphorus Loadings 1965–2009. Kingston, Ontario, Canada.

Lamon III, E.C., Carpenter, S.R., Stow, C.A., 1998. Forecasting PCB concentrations in Lake Michigan salmonids: a dynamic linear model approach. Ecological Applications 8, 659–668.

Leisti, K.E., Millard, E.S., Minns, C.K., 2006. Assessment of Submergent Macrophytes in the Bay of Quinte, Lake Ontario, August 2004, Including Historical Context. Dept. of Fisheris and Oceans, Canada.

Lick, W., 1986. Modeling the transport of fine-grained sediments in aquatic systems. Science of the Total Environment 55, 219–228.

Mehta, A.J., Parchure, T.M., Dixit, J.G., Ariathurai, R., 1982. Resuspension potential of deposited cohesive sediment beds. In: Kennedy, V.S. (Ed.), Estuarine Comparisons. Academic Press, New York, pp. 591–609.

Mian, M.H., Yanful, E.K., 2004. Analysis of wind-driven resuspension of metal mine sludge in a tailings pond. Journal of Environmental Engineering and Science 3, 119–135.

Minns, C.K., Moore, J.E., 2004. Modelling Phosphorus Management in the Bay of Quinte, Lake Ontario in the Past, 1972–2001 and in the Future. Burlington, Ontario.

Minns, C.K., Moore, J.E., Seifried, K.E., 2004. Nutrient Loads and Budgets in the Bay of Quinte, Lake Ontario, 1972–2001. Burlington, Ontario.

Munawar, M., Fitzpatrick, M., Niblock, H., Lorimer, J., 2011. The relative importance of autotrophic and heterotrophic microbial communities in the planktonic food web of the Bay of Quinte, Lake Ontario 2000–2007. Aquatic Ecosystem Health and Management Society 14, 21–32.

Nicholls, K.H., Carney, E.C., 2011. The phytoplankton of the Bay of Quinte, 1972–2008: point-source phosphorus loading control, dreissenid mussel establishment, and a proposed community reference. Aquatic Ecosystem Health and Management Society 14, 33–43.

Nicholls, K.H., Heintsch, L., Carney, E., 2002. Univariate step-trend and multivariate assessments of the apparent effects of P loading reductions and zebra mussels on the phytoplankton of the Bay of Quinte, Lake Ontario. Journal of Great Lakes Research 28, 15–31.

Office of Water, 1997. Guidelines for Preparation of the Comprehensive State Water Quality Assessments. Environmental Protection Agency, Washington, D.C., U.S.

OhioEPA, 2010. Ohio Lake Erie Phosphorus Task Force Final Report: Executive Summary. Columbus, Ohio.

Palmer, M.E., Winter, J.G., Young, J.D., Dillon, P.J., Guildford, S.J., 2011. Introduction and summary of research on Lake Simcoe: research, monitoring and restoration of a large lake and its watershed. Journal of Great Lakes Research 37 (Suppl. 3), 1–6.

Petticrew, E.L., Kalff, J., 1992. Water flow and clay retention in submerged macrophyte beds. Canadian Journal of Fisheries and Aquatic Sciences 49, 2483–2489.

Pole, A., West, M., Harrison, J., 1994. Applied Bayesian Forecasting and Time Series Analysis. Champman & Hall/CRC, Washington, D.C.

Project Quinte members, 2011. Project Quinte Annual Report 2009. Kingston, Ontario, Canada.

Rørslett, B., Berge, D., Johansen, S.W., 1986. Lake enrichment by submersed macrophytes: a Norwegian whole-lake experience with Elodea canadensis. Aquatic Botany 26, 325–340.

Ramin, M., Stremilov, S., Labencki, T., Gudimov, A., Boyd, D., Arhonditsis, G.B., 2011. Integration of numerical modeling and Bayesian analysis for setting water quality criteria in Hamilton Harbour, Ontario, Canada. Environmental Modeling and Software 26, 337–353.

Reckhow, K.H., Arhonditsis, G.B., Kenney, M.A., Hauser, L., Tribo, J., Wu, C., Elcock, K.J., Steinberg, L.J., Stow, C.A., McBride, S.J., 2005. A predictive approach to nutrient criteria. Environmental Science and Technology 39, 2913–2919.

Reichert, P., Omlin, M., 1997. On the usefulness of overparameterized ecological models. Ecological Modeling 95, 289–299.

Repavich, W.M., Sonzogni, W.C., Standridge, J.H., Wedepohl, R.E., Meisner, L.F., 1990. Cyanobacteria (blue-green algae) in Wisconsin waters: acute and chronic toxicity. Water Research 24, 225–231.

Sand-Jensen, K., 1998. Influence of submerged macrophytes on sediment composition and near-bed flow in lowland streams. Freshwater Biology 39, 663–679.

Scheffer, M., Straile, D., van Nes, E.H., Hosper, H., 2001. Climatic warming causes regime shifts in lake food webs. Limnology and Oceanography 46, 1780–1783.

Schneider, D.W., 1992. A bioenergetics model of zebra mussel, Dreissena polymorpha, growth in the Great Lakes. Canadian Journal of Fisheries and Aquatic Sciences 49, 1406–1416.

Seifried, K.E., 2002. Submerged Macrophytes in the Bay of Quinte: 1972–2000. Department of Zoology, University of Toronto, p. 132.

Sprung, M., Rose, U., 1988. Influence of food size and food quantity on the feeding of the mussel Dreissena polymorpha. Oecologia 77, 526–532.

Stow, C.A., Lamon, E.C., Qian, S.S., Schrank, C.S., 2004. Will Lake Michigan lake trout meet the Great Lakes Strategy 2002 PCB reduction goal. Environmental Science and Technology 38, 359–363.

Thornton, K.W., Lessem, A.S., 1978. A temperature algorithm for modifying biological rates. Transactions of the American Fisheries Society 107, 284–287.

Tsai, C.-H., Lick, W., 1986. A portable device for measuring sediment resuspension. Journal of Great Lakes Research 12, 314–321.

Vanderploeg, H.A., Liebig, J.R., Carmichael, W.W., Agy, M.A., Johengen, T.H., Fahnenstiel, G.L., Nalepa, T.F., 2001. Zebra mussel (Dreissena polymorpha) selective filtration promoted toxic Microcystis blooms in Saginaw Bay (Lake Huron) and Lake Erie. Canadian Journal of Fisheries and Aquatic Sciences 58, 1208–1221.

Walz, N., 1978. The energy balance of the freshwater mussel Dreissena polymorpha (Pallas) in laboratory experiments and in Lake Constance: I. Pattern of activity, feeding and assimilation efficiency. Archiv für Hydrobiologie Suppl. 55, 83–105.

Wang, H., Appan, A., Gulliver, J.S., 2003a. Modeling of phosphorus dynamics in aquatic sediments: I—model development. Water Research 37, 3928–3938.

Wang, H., Appan, A., Gulliver, J.S., 2003b. Modeling of phosphorus dynamics in aquatic sediments: II—examination of model performance. Water Research 37, 3939–3953.

Watson, S.B., Borisko, J., Lalor, J., 2011. Bay of Quinte Harmful Algal Bloom Programme L Phase I – 2009. Kingston, Ontario, Canada.

West, M., Harrison, J., 1989. Bayesian Forecasting and Dynamic Models. Springer-Verlag, New York.

Wetzel, R.G., 2001. Limnology. Academic Press, San Diego, CA.

Wigand, C., Stevenson, J.C., Cornwell, J.C., 1997. Effects of different submersed macrophytes on sediment biogeochemistry. Aquatic Botany 56, 233–244.

XCG Consultants Ltd., 2009. Bay of Quinte Remedial Action Plan Advancement of PPCPs for Quinte Municipalities: Analysis of Phosphorus Inputs to the Bay of Quinte from Urban Stormwater Discharges from on-Bay Municipalities. Belleville, ON, Canada.

Zhang, W., Kim, D.-K., Rao, Y., Watson, S., Mugalingam, S., Labencki, T., Dittrich, M., Morley, A., Arhonditsis, G.B. Can simple phosphorus mass balance models guide management decisions? A case study in the Bay of Quinte, Ontario, Canada. Ecological Modeling, 2013, http://dx.doi.org/10.1016/j.ecolmodel.2013.02.023

Zimmer, K.D., Hanson, M.A., Buttler, M.G., 2001. Influences of fathead minnows and aquatic macrophytes on nutrient partitioning and ecosystem structure in two prairie wetlands. Archiv für Hydrobiologie 150, 411–433.

IMPROVING THE REPRESENTATION OF INTERNAL NUTRIENT RECYCLING WITH PHOSPHORUS MASS BALANCE MODELS: A CASE STUDY IN THE BAY OF QUINTE, ONTARIO, CANADA

(Electronic Supplementary Material)

Dong-Kyun Kim[1], Weitao Zhang[1], Yerubandi R. Rao[2], Sue Watson[2],

Shan Mugalingam[3], Tanya Labencki[4], Maria Dittrich[1], Andrew Morley[5],

George B. Arhonditsis[1]*

[1] Ecological Modelling Laboratory

Department of Physical & Environmental Sciences, University of Toronto,

Toronto, Ontario, Canada, M1C 1A4

[2] Environment Canada, National Water Research Institute

Burlington, Ontario, Canada, L7R 4A6

[3] Lower Trent Conservation

Trenton, Ontario, Canada, K8V 5P4

[4] Environmental Monitoring and Reporting Branch, Ontario Ministry of the Environment

Toronto, Ontario, Canada, M9P 3V6

[5] Kingston Regional Office, Ontario Ministry of the Environment

Kingston, Ontario, Canada, K7M 8S5

* Corresponding author

E-mail: georgea@utsc.utoronto.ca, Tel.: +1 416 208 4858; Fax: +1 416 287 7279.

Figures Legends

Figure SI-1: Sensitivity of *TP* simulations on macrophyte light limitation: grey lines: reference simulation; long-dashed line: scenario of light deficiency (α_1=1.25, α_2=0.025), short-dashed line: scenario of optimal illumination of the water column (α_1=0.75, α_2=0.015); dotted line: scenario of increased water clarity coupled with an increase of the optimal solar radiation for macrophyte growth (α_1=0.75, α_2=0.015, I_{opt}=28.5).

Figure SI-2: Sensitivity of *TP* simulations on macrophyte phosphorus limitation: grey lines: reference simulation; dashed line: low affinity for phosphorus (K_p=12.5); dotted line: high affinity for phosphorus (K_p=7.5).

Figure SI-3: Sensitivity of *TP* simulations on phosphorus recycling regimes mediated by macrophytes: grey line: reference simulation; long-dashed line: fast macrophyte growth and metabolic rates and fast sediment decomposition rates (P_m=0.0975, R_{mac20}=0.027, D_{mac}=0.0015, K_{d20}=0.0003); short-dashed line: fast macrophyte growth and metabolic rates and slow sediment decomposition rates (P_m=0.0975, R_{mac20}=0.027, D_{mac}=0.0015, K_{d20}=0.0002); dotted line: slow macrophyte growth and metabolic rates and slow sediment decomposition rates (P_m=0.0325, R_{mac20}=0.009, D_{mac}=0.0005, K_{d20}=0.0002).

Figure SI-4: Sensitivity of TP simulations on different colonization levels of dreissenids: grey lines: reference simulation; dashed line: 20% areal colonization; dotted line: 80% areal colonization.

Figure SI-5: Sensitivity of *TP* simulations on phosphorus recycling regimes mediated by dreissenids: grey lines: reference simulation; dashed line: fast dreissenid ingestion and respiration rates and fast sediment decomposition rates (a_c=0.03875, a_r=0.0025, K_{d20}=0.00025); dotted line: slow dreissenid ingestion and respiration rates and slow sediment decomposition rates (a_c=0.02325, a_r=0.0015, K_{d20}=0.00015).

Figure SI-6: Sensitivity of *TP* simulations on sediment porosity: grey lines: reference simulation; dashed line: high sediment porosity (φ=0.9); dotted line: low sediment porosity (φ=0.7))

Figure SI-7: Sensitivity of *TP* simulations on phosphorus diffusion from the sediments: grey lines: reference simulation; dashed line: high diffusivity with thicker sediments (K_{diff}=0.000875, δ=125%); dotted line: low diffusivity with thinner sediments (K_{diff}=0.000525, δ=75%).

Figures SI-8: Sensitivity of *TP* simulations on phosphorus adsorption/desorption processes in the sediments: grey lines: reference simulation; dashed line: predominance of adsorption fluxes (K_{ad}=5.4, PIP_{max}=1, E=10.925), dotted line: predominance of desorption fluxes (K_{ad}=7.56, PIP_{max}=0.6, E=9.025).

Figures SI-9: Simulated *TP* concentrations at the segments U_2 and U_3 in the upper Bay of Quinte. The first eight years of each simulation are based on the actual meteorological and loading forcing during the 2002-2009 period, while the following ten years (2010-2019) are forced with constant flows (i.e., 500 m^3 s^{-1}) and *TP* riverine concentrations (i.e., 20 µg L^{-1}).
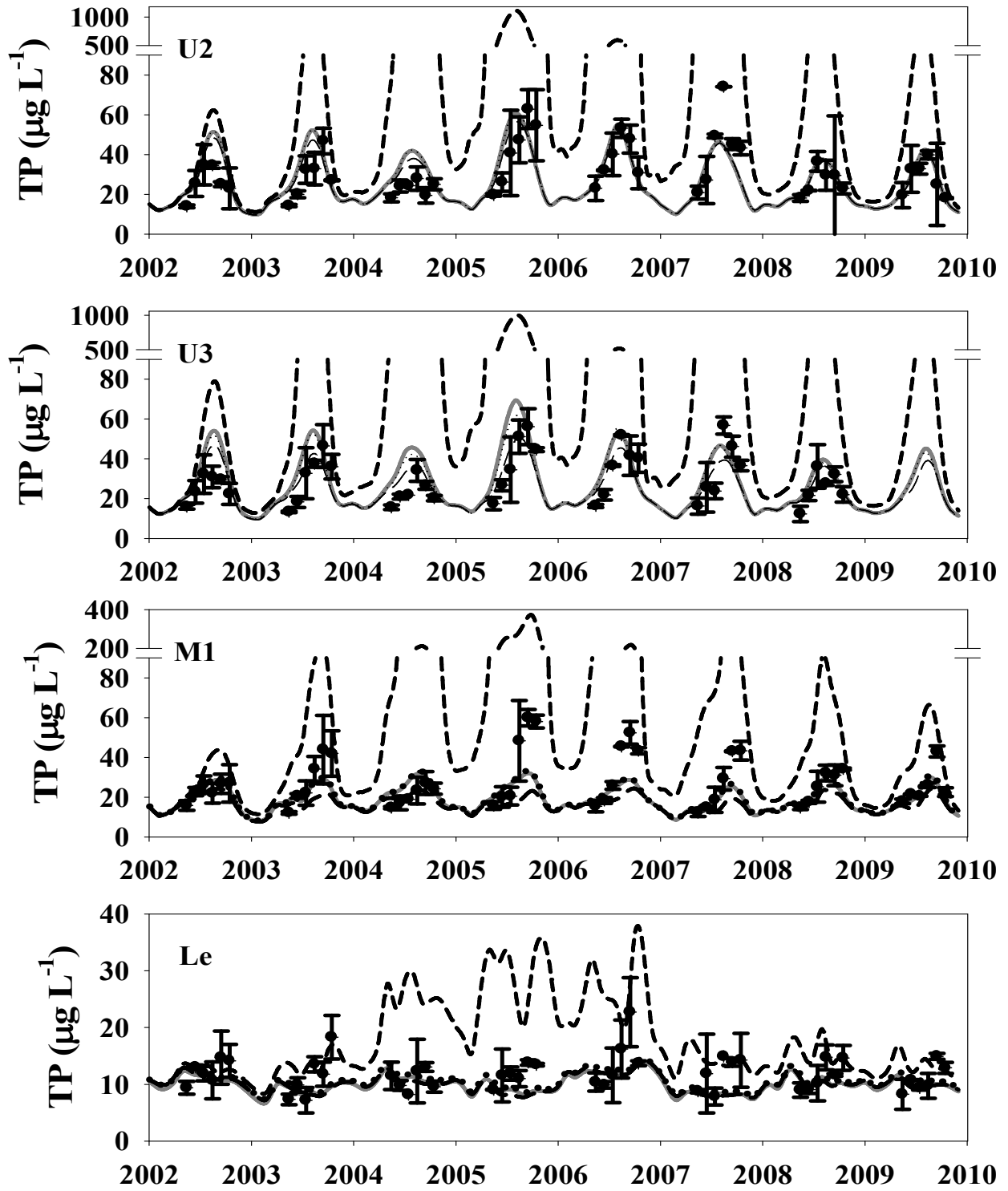
Figure SI-1

Figure SI-2

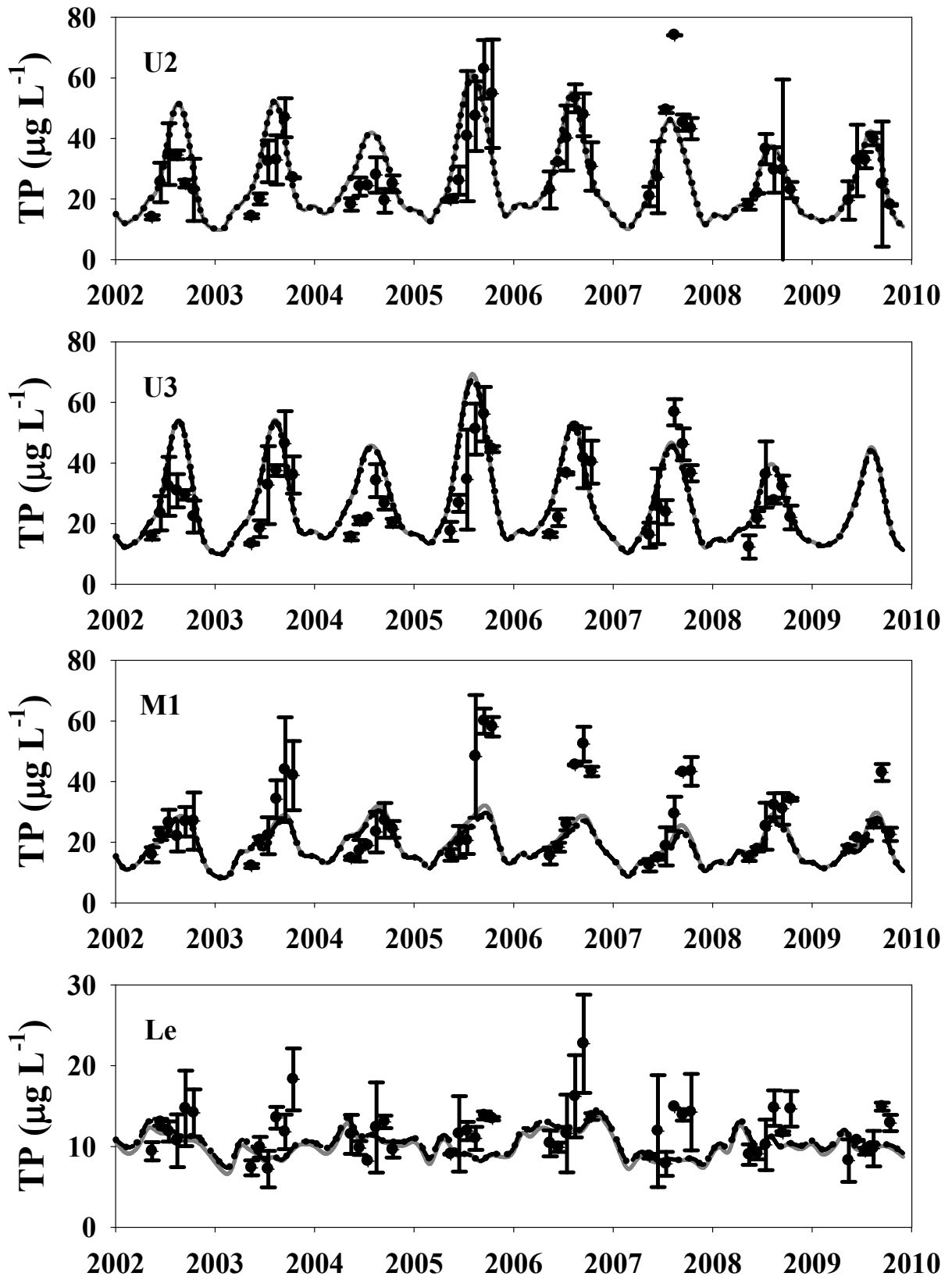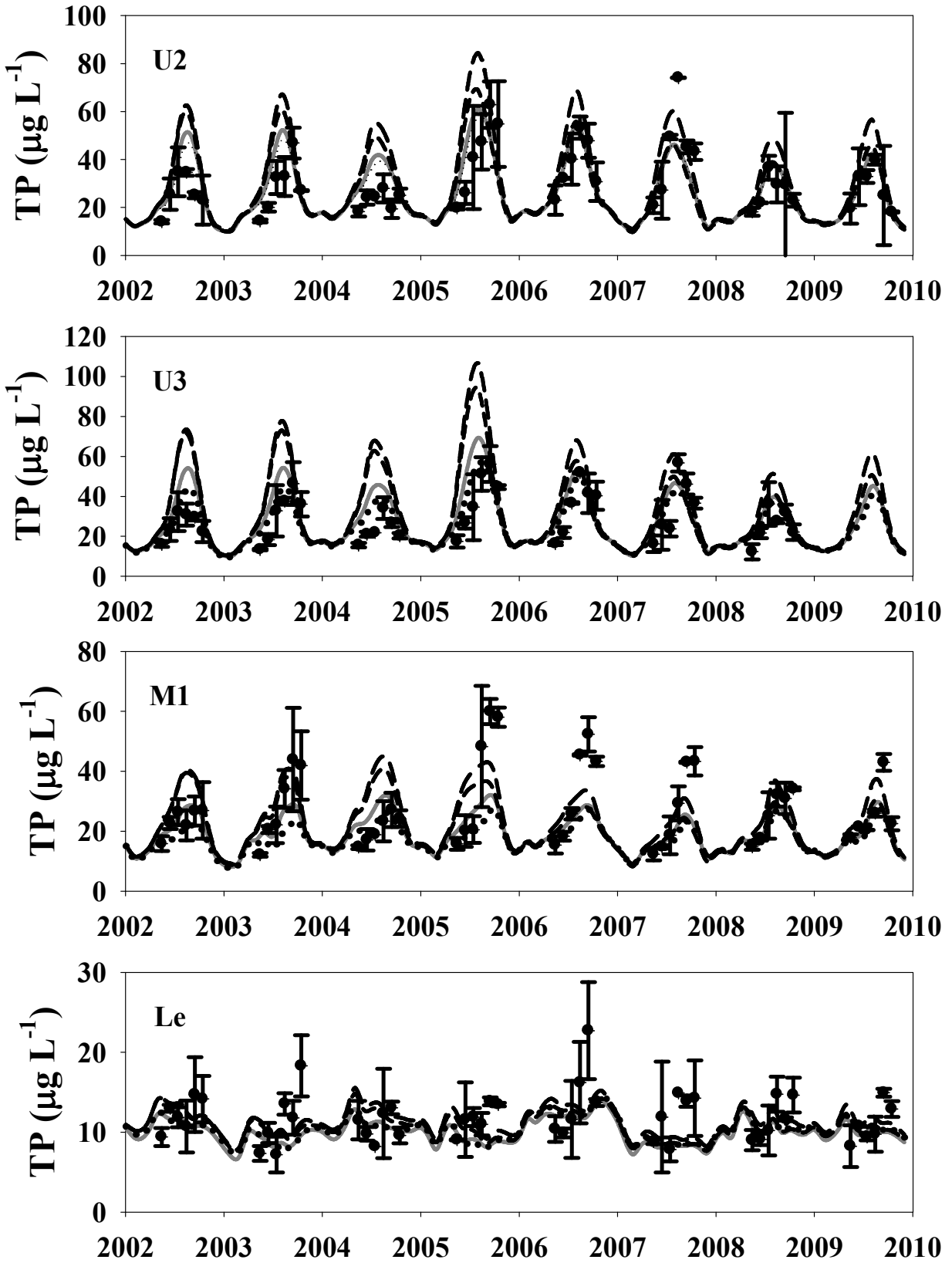**Figure SI-3**
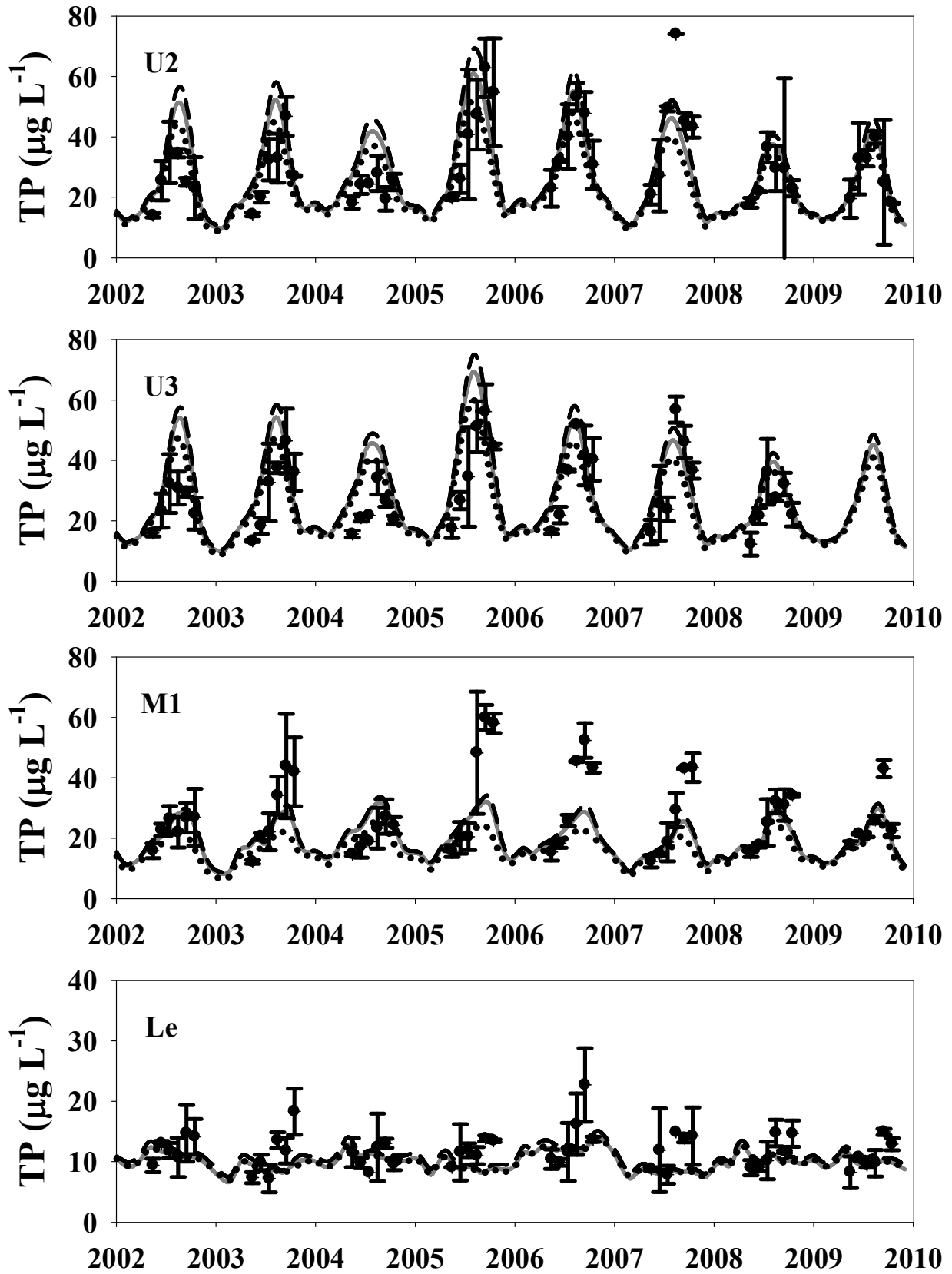
Figure SI-4
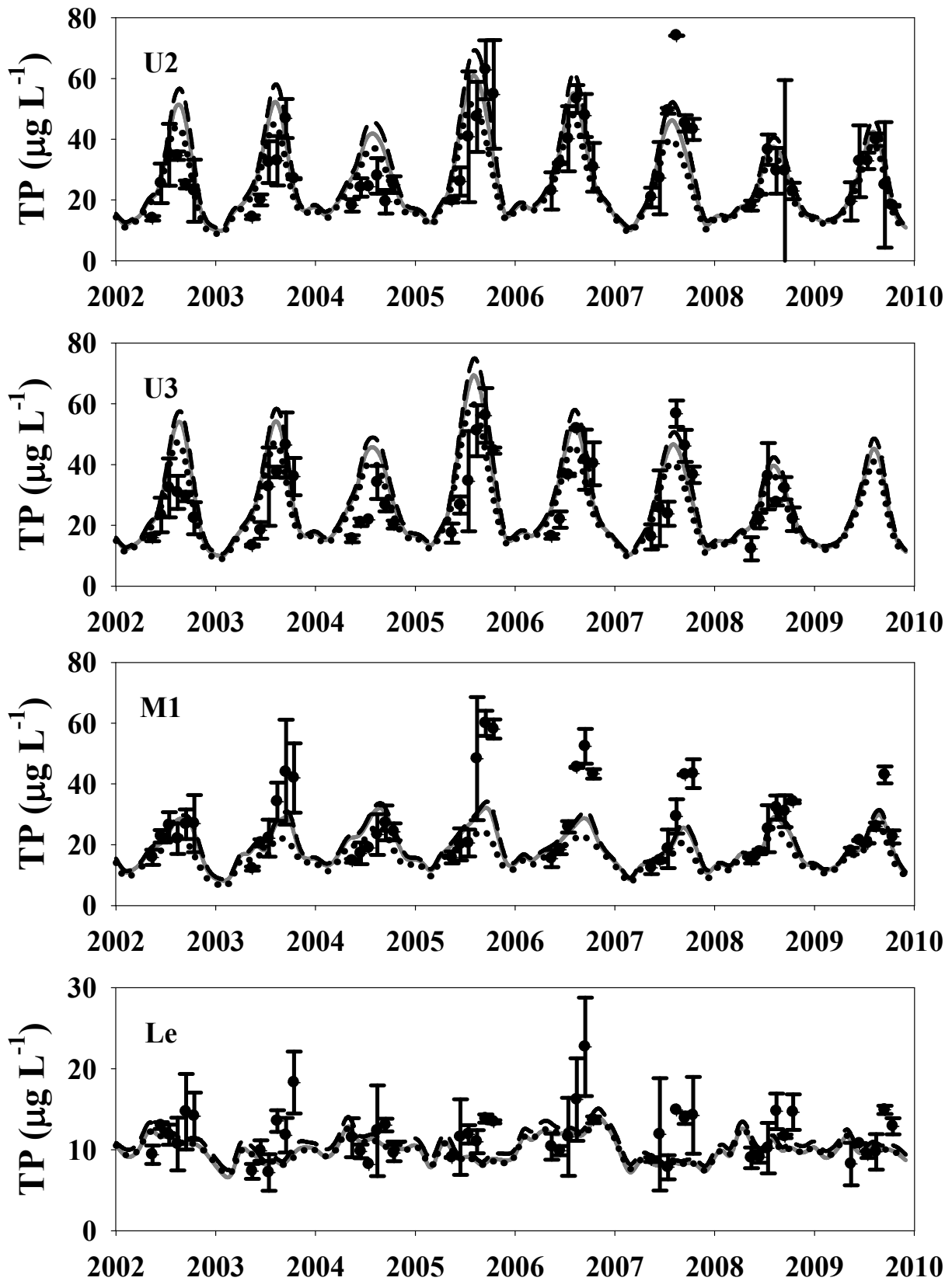
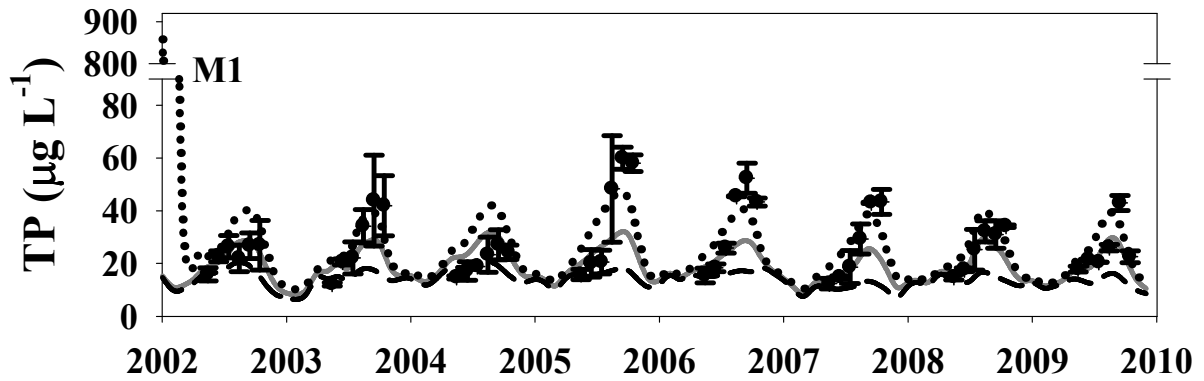**Figure SI-5**
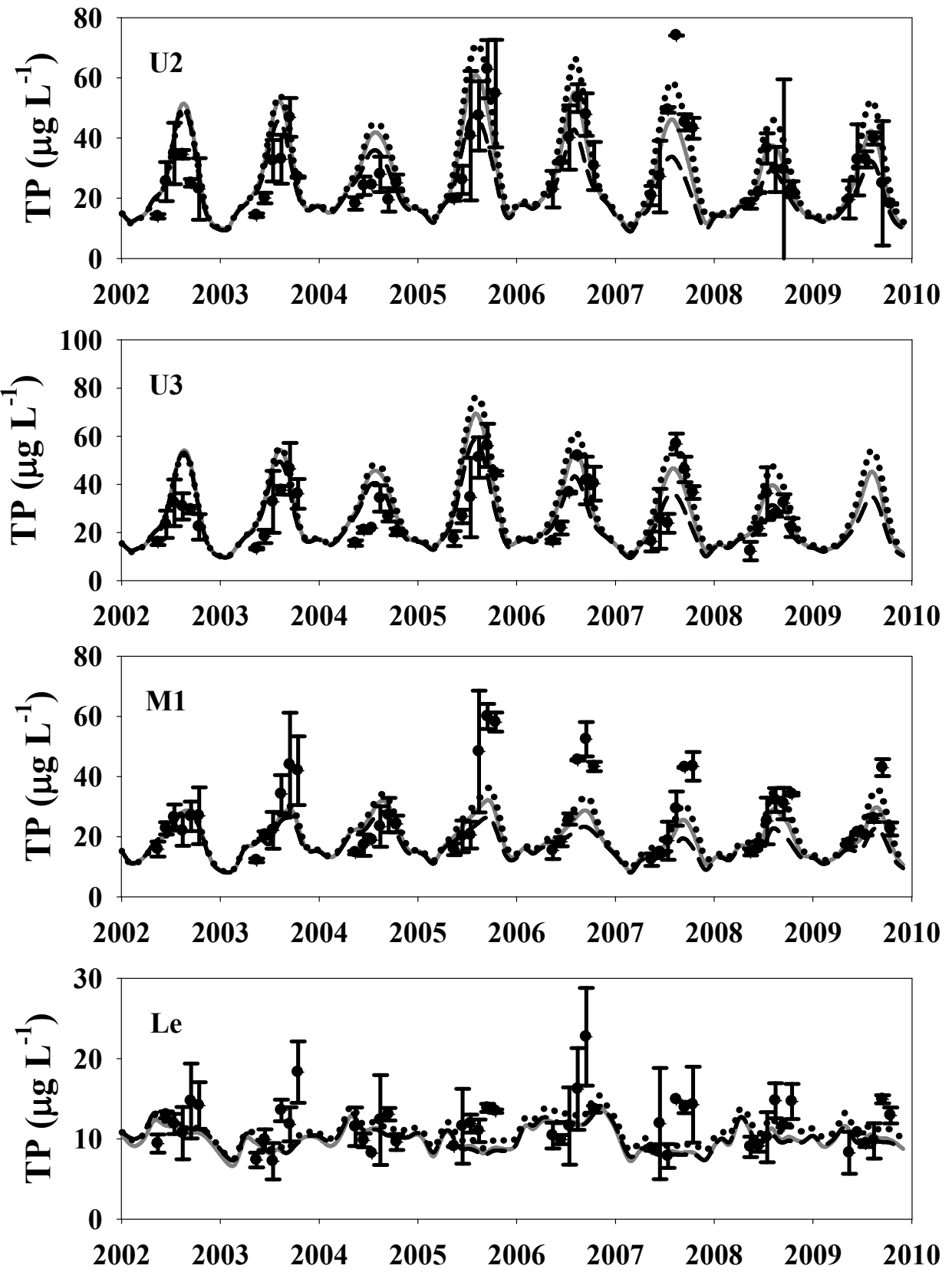
Figure SI-6
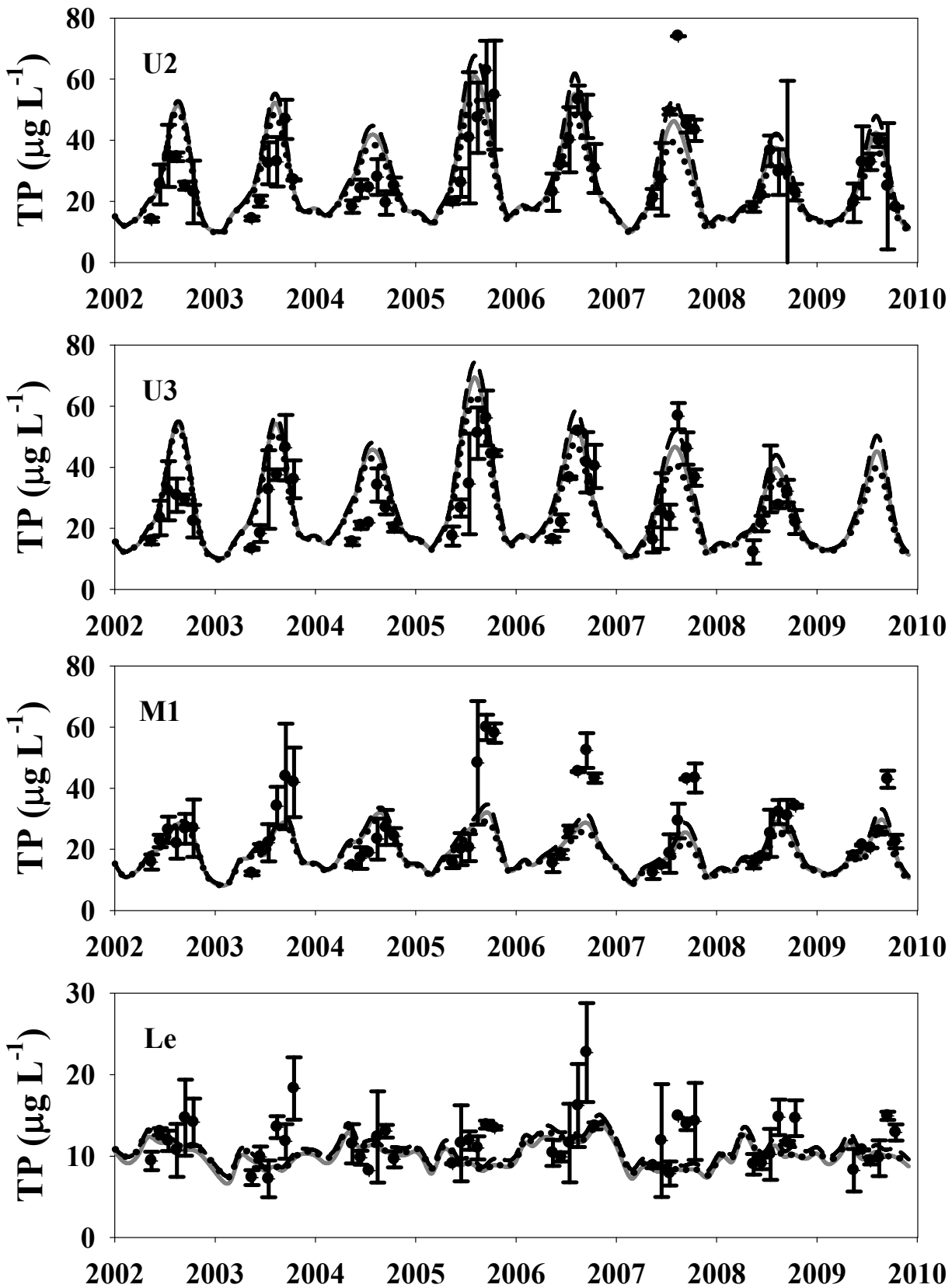
Figure SI-7
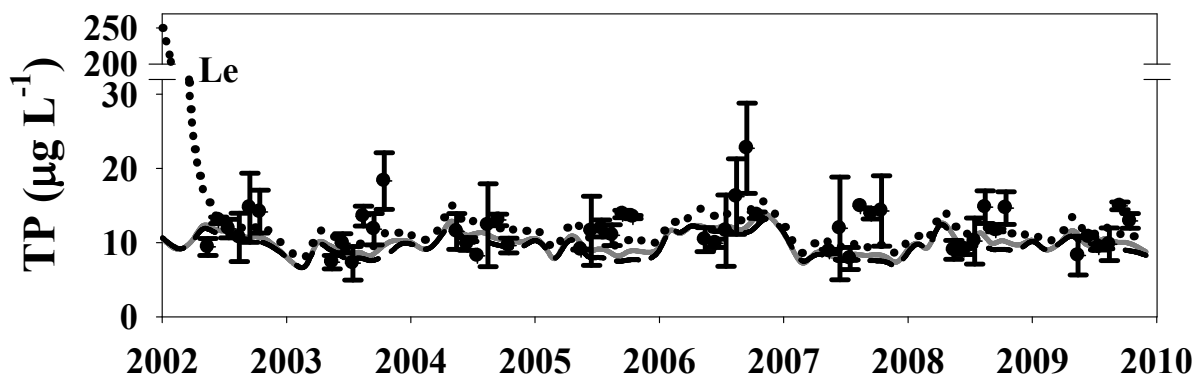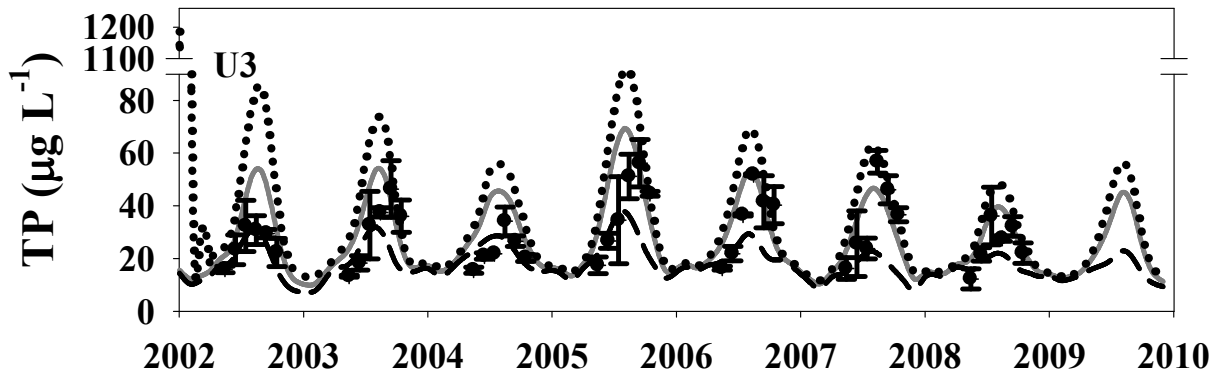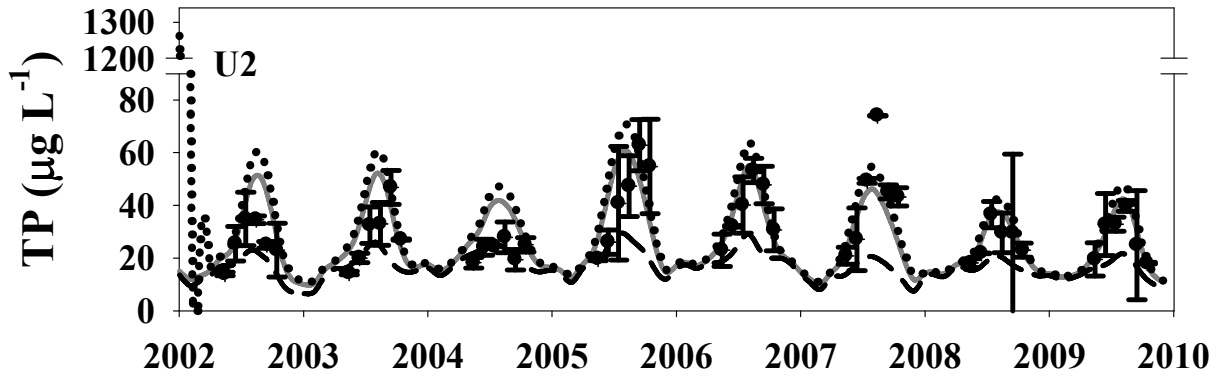
Figure SI-8
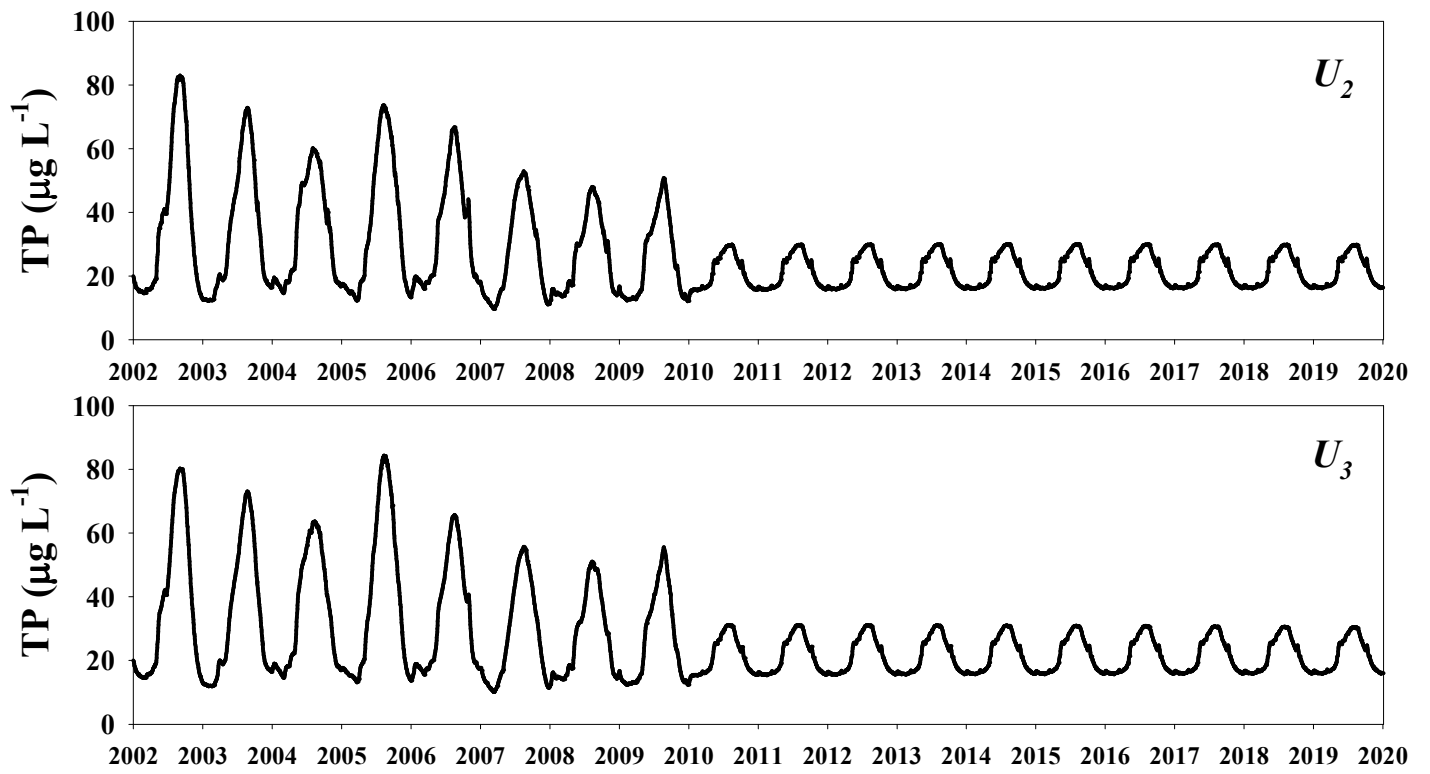
Figure SI-9

Table SI-1. Mathematical equations of the total phosphorus model.

Process	*Symbol*	*Equation*
Water column	$\dfrac{dTP_w}{dt}$	$TP_{in} + TP_{sdR} + TP_{sdD} + TP_{macR} + TP_{zmR} + TP_{zmX} - TP_{out} - TP_{wS} - TP_{zmF} + [TP_{backflow} + TPD_{Le.Lh}]$
	TP_{sdR}	$\dfrac{A}{V_w} R_{resus}$
	TP_{sdD}	$D_{sed}(DIP_{sed} - DIP_w)$
	TP_{macR}	$\alpha_{mac} \cdot \dfrac{A}{V_w} \cdot (R_{mac} \cdot BP_{mac}) \cdot B_{mac}$
	TP_{zmR}	$\alpha_{zm} \cdot \dfrac{A}{V_w} \cdot BP_{zm} w_r R_{zm} B_{zm}$
	TP_{wS}	$\dfrac{V_s}{z} \cdot TP_w$
	V_s	$V_{s1} \cdot \dfrac{TP_w - P_{phyt}}{TP_w} + V_{s2} \cdot \dfrac{P_{phyt}}{TP_w}$
	P_{phyt}	$(0.6115 \cdot TP_w - 5.4923) \cdot P/chla$
	TP_{zmF}	$\dfrac{FT_{zm}}{V_w}$
	TP_{zmX}	$\alpha_{zm} \cdot \dfrac{A}{V_w} \cdot BP_{zm}(1 - f_{OP-ZM}) \cdot w_f U_{zm} B_{zm}$
	$TPD_{Le,Lh}$	$\dfrac{1}{V_{Le,Lh}(t)}\left[A_{Lh}\left\{\dfrac{K_{(str/nstr)}(\Delta TP_{Le/Lh})}{\Delta z}\right\}\right]$
Macrophytes	$\dfrac{dB_{mac}}{dt}$	$(G_{mac} - R_{mac} - D_{mac}) \cdot B_{mac}$
	G_{mac}	$P_m \dfrac{DIP_{sed}}{K_p + DIP_{sed}} f_L(t)$
	$f_L(t)$	$\dfrac{2.718\ FD}{K_{ext}\ Z_{mac}} \{e^{x1} - e^{x2}\}$
	$x1$	$\dfrac{I_0 e^{-K_{ext}Z_{mac}}}{FD\ I_{opt}}$
	$x2$	$\dfrac{I_0}{FD\ I_{opt}}$
	K_{ext}	$\alpha_1 + \alpha_2 chla$
	R_{mac}	$R_{mac20} \cdot \theta_{rmac}^{(T-20)}$

Dreissenids	$\dfrac{dB_{zm}}{dt}$	$(w_f I_{zm} - (w_r R_{zm} + w_f F_{zm} + w_f U_{zm})) B_{zm}$
	I_{zm}	$a_c B_{zm}{}^{b_c} \cdot f_I(t) \cdot \min\left(\dfrac{PP_w}{K_{cp}}, 1\right)$
	$f_I(t)$	$\dfrac{K_1 e^{\gamma_1(t-t_1)}}{1 + K_1(e^{\gamma_1(t-t_1)} - 1)} \cdot \dfrac{K_4 e^{\gamma_2(t_4-t)}}{1 + K_4(e^{\gamma_2(t_4-t)} - 1)}$
	γ_1	$\dfrac{1}{t_2 - t_1} \cdot \ln \dfrac{K_2(1 - K_1)}{K_1(1 - K_2)}$
	γ_2	$\dfrac{1}{t_4 - t_3} \cdot \ln \dfrac{K_3(1 - K_4)}{K_4(1 - K_3)}$
	R_{zm}	$a_r B_{zm}{}^{b_r} \cdot f_r(t) + \dfrac{w_f}{w_r} \cdot SDA(I_{zm} - F_{zm})$
	$f_r(t)$	$V^x e^{x(1-V)}$
	V	$\dfrac{t_m - t}{t_m - t_0}$
	x	$\left(\dfrac{w\left(1 + \sqrt{1 + 40/y}\right)}{20}\right)^2$
	w	$\ln Q(t_m - t_0)$
	y	$\ln Q(t_m - t_0 + 2)$
	PP_w	$TP_w(1 - w_{DIP})$
	F_{zm}	$\alpha_f \exp\left(\gamma_f \cdot \min\left(\dfrac{PP_w}{K_{cp}}, 1\right)\right) \cdot I_{zm}$
	U_{zm}	$\alpha_u(I_{zm} - F_{zm})$
	FR	$\dfrac{\alpha_c}{K_{cp} \cdot 0.34} \quad \text{if } PP_w < K_{cp}$ $\dfrac{\alpha_c}{PP_w \cdot 0.34} \quad \text{if } PP_w > K_{cp}$
	FT_{zm}	$FR \cdot B_{zm} \cdot \alpha_{zm} \cdot A \cdot PP_w$
Dissolved Inorganic Phosphorus	$\dfrac{dDIP_{sed}}{dt}$	$-D_{sed}(DIP_{sed} - DIP_w) + S_{sed}(DIP_{sede} - DIP_{sed}) + K_{decom} \cdot \dfrac{\rho}{\varphi} \cdot OP_{sed} - G_{mac} \cdot a_{mac} \cdot \left(\dfrac{A}{\varphi V_{sed}}\right) \cdot B_{mac}$ $\cdot BP_{mac}$
	D_{sed}	$\theta_s^{T-20} \cdot \dfrac{K_{DO}}{K_{DO} + DO} \cdot \dfrac{\varphi K_{diff}}{\delta^2}$
	S_{sed}	φK_{ad}
	DIP_{sede}	$\dfrac{PIP_{sed}}{E \cdot (PIP_{max} - PIP_{sed})}$
	K_{decom}	$K_{d20} \cdot \theta_s^{T-20}$

Particulate Inorganic Phosphorus	$\dfrac{dPIP_{sed}}{dt}$	$-f_{resus} \cdot \dfrac{A}{\rho \cdot V_{sed}} R_{resus} - S_{sed}(DIP_{sede} - DIP_{sed}) \cdot \dfrac{\varphi}{\rho} - B_{sed-PIP} \cdot PIP_{sed}$
	B_{sed-PP}	$\dfrac{S_{bur}}{\delta}$
Organic Phosphorus	$\dfrac{dOP_{sed}}{dt}$	$\dfrac{V_s \cdot TP_w}{z} \cdot \dfrac{A}{\rho \cdot V_{sed}} - (1 - f_{resus}) \cdot \dfrac{A}{\rho \cdot V_{sed}} \cdot R_{resus} - B_{sed-PP} \cdot OP_{sed} - K_{decom} \cdot OP_{sed} + D_{mac} \cdot B_{mac}$
		$\cdot \dfrac{\alpha_{mac} \cdot A}{\rho \cdot V_{sed}} \cdot BP_{mac} + D_{zm} \cdot B_{zm} \cdot \dfrac{\alpha_{zm} \cdot A}{\rho \cdot V_{sed}} \cdot BP_{zm} + \dfrac{Psdf_{zm}}{\rho \cdot V_{sed}}$
	D_{zm}	$w_f \cdot (f_{OP-ZM} \cdot U_{zm} + F_{zm})$
	$Psdf_{zm}$	$FT_{zm} - w_f \cdot I_{zm} \cdot A \cdot B_{zm} \cdot BP_{zm}$
Sediment resuspension	R_{resus}	$a_{sdR} \left(\dfrac{\tau - \tau_c}{\tau_c} \right)^{b_{seR}} \quad \text{if } \tau \geq \tau_c \;, \quad 0 \quad \text{if } \tau < \tau_c$

Table SI-2. State variables and parameters of the TP model.

Symbol	Variables and Parameters	Value	Unit
A	Segment area		m^2
A_{Lh}	Epilimnion/Hypolimnion interface		m^2
b_c	Exponent for weight effect on dreissenid ingestion	-0.39	
B_{mac}	Macrophyte biomass (dry weight)		$g\ m^{-2}$
BP_{mac}	Phosphorus content in macrophyte biomass	0.0025	$g\ P\ g\ dry\ weight^{-1}$
BP_{zm}	Phosphorus content in dreissenid biomass	0.01	$g\ P\ g\ dry\ weight^{-1}$
b_r	Exponent for weight effect on respiration	-0.25	
b_{sdR}	Sediment bed shear stress exponent	1	
B_{sed-PP}	Burial rate of particulate phosphorus		day^{-1}
B_{zm}	Dreissenid biomass		$g\ /\ m^2$
$chla$	Chlorophyll a concentration		$\mu g\ L^{-1}$
DIP_{sed}	DIP in the sediments		$\mu g\ L^{-1}$
DIP_{sede}	Equilibrium phosphorus concentration in the solid phase of sediments		$\mu g\ L^{-1}$
DIP_w	DIP in the water column		$\mu g\ L^{-1}$
D_{mac}	Macrophyte mortality rate	0.001	day^{-1}
DO	Dissolved oxygen concentration		$mg\ O_2\ L^{-1}$
D_{sed}	Diffusion exchange rate between sediment pore water and water column		day^{-1}
D_{zm}	Dreissenid egestion and excretion		$g\ food\ g\ mussel^{-1}\ day^{-1}$
E	Langmuir sorption constant	9.5	$L\ mg^{-1}$
FD	Time fraction of daily solar radiation		
$f_I(t)$	Temperature dependence of ingestion		
f_{OP-ZM}	Fraction of organic phosphorus in dreissenid excretion	0.6	
FR	Dreissenid filtration rate		$L\ g\ mussel^{-1}\ day^{-1}$
$f_r(t)$	Temperature dependence of respiration		
f_{resus}	Inorganic fraction of resuspended phosphorus	0.5	
FT_{zm}	Phosphorus mass filtered by dreissenids		$kg\ day^{-1}$
F_{zm}	Dreissenid egestion		$g\ food\ g\ mussel^{-1}\ day^{-1}$
G_{mac}	Macrophyte growth rate		day^{-1}
I_o	Solar radiation on the surface		$MJ\ m^{-2}\ day^{-1}$
I_{opt}	Optimal solar radiation for macrophyte growth	18	$MJ\ m^{-2}\ day^{-1}$
I_{zm}	Dreissenid food ingestion		$g\ food\ g\ mussel^{-1}\ day^{-1}$
K_1	Empirical coefficient representing temperature effect on ingestion at t_1	0.1	
K_2	Empirical coefficient representing temperature effect on ingestion at t_2	0.98	
K_3	Empirical coefficient representing temperature effect on ingestion at t_3	0.98	
K_4	Empirical coefficient representing temperature effect on ingestion at t_4	0.02	
K_{ad}	First-order desorption/sorption rate	7.2	day^{-1}
K_{cp}	Saturation particulate phosphorus concentration	50	$\mu g\ P\ L^{-1}$
K_{d20}	Decomposition rate coefficients at 20 °C	0.0002 (0.00018**)	day^{-1}
K_{decom}	Sediment decomposition rate		day^{-1}
K_{diff}	Sediment diffusion exchange at reference temperature (20 °C)	0.0007 (0.0003**)	$m^2\ day^{-1}$
K_{DO}	Half saturation constant for anaerobic phosphorus sediment release	0.5	$mg\ O_2\ L^{-1}$
K_{nstr}	Diffusivity in non-stratified conditions	10	$m^2\ day^{-1}$
K_p	Half saturation constant for phosphate in sediment pore water	10 (8.5**)	$\mu g\ L^{-1}$
K_{str}	Diffusivity in stratified conditions	0.15	$m^2\ day^{-1}$
OP_{sed}	Organic phosphorus in the sediments		$mg\ g^{-1}$

Symbol	Description	Value	Units
$P/chla$	Phosphorus to chlorophyll a ratio	1.218	$\mu g\ P\ \mu g\ chla^{-1}$
PIP_{max}	Maximum sorption capacity	0.8	$mg\ g^{-1}$
PIP_{sed}	PIP in the sediments		$mg\ g^{-1}$
P_m	Maximum gross photosynthesis rate	0.065 (0.052**)	day^{-1}
P_{phyt}	Phosphorus in the water column sequestered in phytoplankton		$\mu g\ P\ L^{-1}$
PP_w	Particulate phosphorus in water		$\mu g\ L^{-1}$
$Psdf_{zm}$	Pseudofecal mass from dreissenids		$kg\ day^{-1}$
Q	Slope estimate, approximately Q_{10}	3.1	
R_{mac}	Macrophyte respiration rate		day^{-1}
R_{mac20}	Macrophyte respiration rate at 20°C	0.018 (0.0142**)	day^{-1}
R_{resus}	Sediment resuspension rate		$kg\ day^{-1}$
R_{zm}	Dreissenid respiration		$g\ O_2\ g\ mussel^{-1}\ day^{-1}$
S_{bur}	Burial coefficient	$5.86 \times 10^{-6}\ (1\times10^{-6}**)$	$m\ day^{-1}$
SDA	Fraction of ingestion spent on feeding energy	0.285	
S_{sed}	Sediment desorption/sorption rate		day^{-1}
T	Water temperature		$°C$
t_0	Optimum temperature for standard respiration	28	$°C$
t_1	Lower temperature at which consumption is K_1 x maximum ingestion	2	$°C$
t_2	Lower temperature at which consumption is K_2 x maximum ingestion	12	$°C$
t_3	Higher temperature at which consumption is K_3 x maximum ingestion	21	$°C$
t_4	Higher temperature at which consumption is K_4 x maximum ingestion	32	$°C$
t_m	Maximum temperature for standard respiration	31	$°C$
$TP_{backflow}$	Total phosphorus fluxes through backflow transport		$\mu g\ L^{-1}\ day^{-1}$
$TPD_{Le,Lh}$	Total phosphorus exchanges between epilimnion and hypolimnion		
TP_{in}	Total phosphorus fluxes from exogenous sources and antecedent segments		$\mu g\ L^{-1}\ day^{-1}$
TP_{macR}	Total phosphorus fluxes from macrophyte respiration		$\mu g\ L^{-1}\ day^{-1}$
TP_{out}	Total phosphorus outflow fluxes		$\mu g\ L^{-1}\ day^{-1}$
TP_{sdD}	Total phosphorus fluxes from sediment diffusion		$\mu g\ L^{-1}\ day^{-1}$
TP_{sdR}	Total phosphorus fluxes from resuspension		$\mu g\ L^{-1}\ day^{-1}$
TP_{sdX}	Total phosphorus fluxes from dreissenid excretion		$\mu g\ L^{-1}\ day^{-1}$
TP_w	Total phosphorus concentration in the water column		$\mu g\ L^{-1}$
TP_{wS}	Total phosphorus settling		$\mu g\ L^{-1}\ day^{-1}$
TP_{zmF}	Total phosphorus filtration		$\mu g\ L^{-1}\ day^{-1}$
TP_{zmR}	Total phosphorus fluxes from dreissenid respiration		$\mu g\ L^{-1}\ day^{-1}$
U_{zm}	Dreissenid excretion		$g\ food\ g\ mussel^{-1}\ day^{-1}$
V_s	Settling rate during the non-growing season (Nov. ~ Apr.)	0.113	$m\ day^{-1}$
V_{s1}	Settling rate of non-algal suspended solids during the growing season	0.1	$m\ day^{-1}$
V_{s2}	Settling rate of phytoplankton during the growing season	0.02	$m\ day^{-1}$
V_{sed}	Segment-specific sediment volume		m^3
V_w	Segment-specific volume as a function of time, determined by the water balance		m^3
w_{DIP}	Proportion of ambient dissolved phosphorus		
w_f	Conversion efficiency	1.724138	$g\ mussel\ g\ food^{-1}$
w_r	Respiration efficiency	5.586207	$g\ mussel\ g\ O_2^{-1}$
z	Water depth		m
Z_{mac}	Water depth from the surface to the top of macrophyte bed	4.3	m
α_1	Background extinction coefficient	1	m^{-1}
α_2	Phytoplankton self-shading effect	0.02	$m^2\ mg\ chla^{-1}$
α_c	Maximum dreissenid ingestion rate	0.031	$g\ food\ g\ mussel^{-1}\ day^{-1}$
α_f	Minimum fraction of food egested	0.315 (0.079*)	

α_{mac}	Segment-specific fraction of macrophyte areal coverage		%
α_r	Maximum dreissenid respiration rate	0.002	$g\ O_2\ g\ mussel^{-1}\ day^{-1}$
α_{sdR}	Resuspension coefficient	8	$mg\ P\ m^2\ day^{-1}$
α_u	Fraction of assimilated food excreted	0.064	
α_{zm}	Segment-specific fraction of dreissenid areal colonization		%
γ_f	Coefficient for egestion dependence on food availability	0.88 (0.22*)	
δ	Sediment thickness at U1, U2, U3 and M2	20	cm
	Sediment thickness at M2 and M3	15	cm
	Sediment thickness at Le and Lh	10	cm
$\Delta TP_{Le/Lh}$	TP gradient between epilimnion and hypolimnion		$\mu g\ L^{-1}$
Δz	Distance between epilimnion and hypolimnion centroids		m
θ_d	Temperature coefficient for decomposition	1.08	
θ_{rmac}	Temperature dependence of macrophyte respiration	1.08	
θ_s	Temperature dependence of sediment diffusion	1.08	
v_{sdR}	Sediment resuspension mass		$kg\ m^{-2}\ day^{-1}$
ρ	Sediment solid density	2.45	$g\ cm^{-3}$
τ	Sediment bed shear stress		$N\ m^{-2}$
τ_c	Critical sediment bed shear stress	0.03	$N\ m^{-2}$
φ	Sediment porosity	0.8	

* Dreissenid characterization that postulates more efficient feeding habits and lower dependence on food availability in the lower segment of the Bay of Quinte.

** Model parameterization based on the assumption that the current estimates underestimate by half the actual *TP* loading during the 2002-2009 period.